Development of an Optimal Xeno-Free cGMP Growth Medium for the Culture of Corneal Stroma-Derived Mesenchymal Stem Cells

Melis Ekrem, BSc (Hons)

Thesis submitted for the degree of Master of Research

University of Nottingham

30th October 2019

Abstract

The characteristic profile of CS-MSCs (Corneal Stroma Derived Mesenchymal Stem Cells) is growing in accordance with their increasing therapeutic interest. *In vitro* expansion of these cells involves basal media DMEM/F-12 supplemented with 10% FBS (Foetal Bovine Serum) or 10% HPL (Human Platelet Lysate). As animal derived serum can confer a risk of disease transmission, and is subject to batch to batch variability, this does not comply with cGMP (current Good Manufacturing Practice) required animal component – free culture protocols for clinical translation. CS-MSCs were additionally cultured in xeno-free and chemically defined media: Stem X Vivo, StemPro MSC SFM XF, Mesenchymal XF and StemMACS XF to determine whether CS-MSCs were able to proliferate at higher levels than in HPL medium and to aid the development of an optimal xeno-free growth media. CS-MSCs cultured in HPL were further subject to comparison with BM-MSCs (Bone Marrow Derived Mesenchymal Stem Cells) cultured in HPL media to assess MSC characteristics and to highlight which media could be determined as most successful for cell proliferation and morphology.

Methods

This project investigated animal-free alternatives to FBS for cultivation of CS-MSCs. CS-MSCs were isolated from human corneal-scleral rims and cultured in either FBS, HPL, Stem X Vivo, StemPro MSC SFM XF, Mesenchymal XF and StemMACS XF media. Cells were characterised using a variety of methods including: Phase Contrast Imaging, Flow Cytometry, Immunocytochemistry, Presto Blue Cell Viability, Cytotoxicity, Enzyme Linked Immunosorbent Assays (ELISAs) and RT-qPCR.

Results

CS-MSCs maintain a MSC phenotype when cultured in FBS and HPL with no differences in phenotypic marker expression or cell viability. CS-MSCs cultured in Stem X Vivo showed higher levels of cell proliferation, marker expression and relative fluorescence when compared to HPL, StemPro MSC SFM XF, Mesenchymal XF and StemMACS XF media. CS-MSCs and BM-MSCs cultured in HPL and xeno-free media did not adhere to tissue culture plastic without the use of bovine gelatine. In addition to this, cell proliferation and viability was significantly lower in BM-MSCs than CS-MSCs cultured in HPL media.

Conclusions

As there is no difference between CS-MSC proliferation between FBS and HPL, HPL should be used as a cell culture media towards a step for clinical translation. It can be concluded that from this project, Stem X Vivo was the best xeno-free media to use for the culture of CS-MSCs. Cell culture using a xeno-free alternative to bovine gelatine requires investigation for progression towards true clinical

translation. This would allow a comprehensive investigation into culturing CS-MSCs and allow phenotypic comparison with BM-MSCs in a true xeno-free culture media.

Acknowledgments

I would like to acknowledge my supervisors; Dr Laura Sidney and Dr Andrew Hopkinson for their guidance, support and friendship throughout this project. I would also like to say a huge thank you to everyone in Academic Ophthalmology who have been the most supportive department throughout my time at Nottingham. You have helped me become a better scientist which I am truly grateful for and I can't wait for the next chapter to begin.

To my family, my parents and my grandparents who have supported me throughout a difficult the year.

Lastly I would like to thank Adam, you have kept me going throughout the year and inspire me every day to be the best that I can be.

Table of Contents

1 Introduction

1.1 The Cornea

The cornea is a highly organised transparent structure located at the ocular surface. It encompasses two functions; to focus light onto the retina and to act as a barrier that protects the interior structures of the eye from exposure to microorganisms [1],[2],[3]. The human cornea is arranged into five layers with distinct regeneration capabilities [4]. These layers consist of the epithelium, Bowman's layer, stroma, Descemet's membrane, and the endothelium [Figure 1]. In 2013 an additional sixth layer, Dua's layer (also known as the Pre-Descemet's Layer), was discovered at the posterior stroma [5]. Trauma to any of the distinct layers can lead to the loss of corneal function and result in visual impairment or blindness [6]. Therefore, the cellular and structural organisation of the human cornea is extremely important for clear vision.

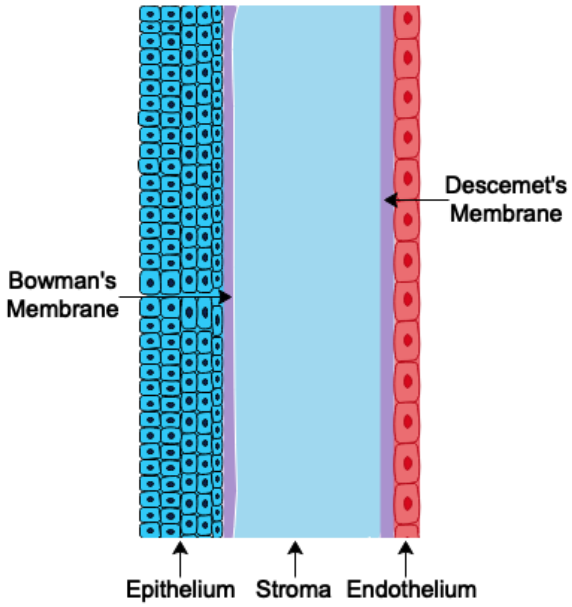

Figure 1: The cross section of a human cornea. The diagram illustrates the five distinct layers of the human cornea which is approximately 550 µm thick.

The cornea is avascular at all stages of development and any abnormal vascularisation from disease or chemical trauma can impair vision. The cornea overcomes this issue in numerous ways. The corneal limbus can be found at the border between the cornea and the white opaque sclera which constitutes of the palisades of Vogt; harbouring the corneal epithelial stem cell niche [Figure 2] [7].

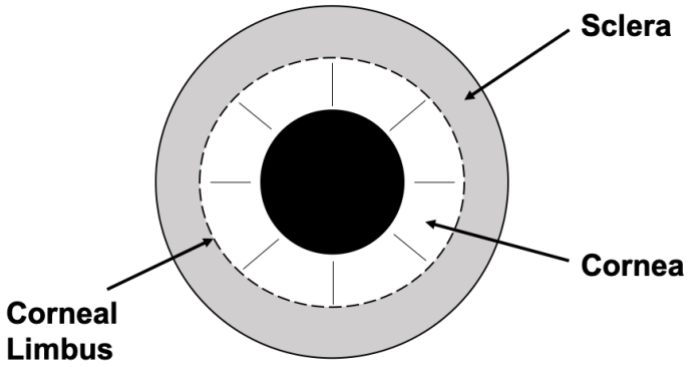

Figure 2: Schematic of the ocular surface. The diagram shows the anterior ocular surface with the limbus in between the cornea and the sclera.

The cornea receives its nutrition directly from the aqueous humour, via the corneal endothelium which is actively pumped into the stroma [8]. The corneal endothelium is responsible for maintaining corneal hydration and transparency via its pumping mechanism (which prevents corneal swelling), whilst the tear film prevents the anterior surface of the eye from dehydration. The tear film consists of antimicrobial components which compensate for the lack of blood – based immunity [9]. Despite the avascular nature of the cornea, the metabolic requirements of the cells must be met. The cornea receives its oxygen supply via the outer capillary network of the limbus and respires primarily through the anterior surface [10].

1.1.1 Immune Privilege

As the anterior surface of the eye lacks vascularisation, this is an initial indication that the cornea encompasses immune privilege [11]. This relationship was originally discovered by Sir Peter Medawar in 1940. Despite ocular immune privilege appearing to be simple, research has shown that it is a highly complex system and thus is yet to be completely understood [12]. Corneal transplant rejection has also been demonstrated to survive indefinitely within the anterior of the eye in contrast to rejection in other tissues and organs such as the skin [11]. During trauma or disease to the cornea, vascular leakage within the anterior chamber of the eye is responsible for triggering transplant rejection. This can lead to widespread transplant rejection throughout the body [12].

Expression of MHC class I and II molecules at the corneal cellular level is relatively low [13]. This indicates that transplanting corneal tissue would induce a weak reaction; the site of engraftment is incapable of generating a strong response. Ocular immune privilege is comprised of three main components: the distinctive anatomical structure of the eye; the expression of immunosuppressive factors; and the unique antigen-specific tolerance; Anterior Chamber - Associated Immune Deviation

(ACAID). ACAID is the systemic immune response triggered by the introduction of antigens into the anterior chamber of the eye [11]. However, as this response is defensive, it does not give rise to a reaction that would cause transplantation rejection [14].

1.1.2 Corneal Nerve

The human cornea was originally thought to be entirely without nerves until Vincent Bochdalek dissected the corneal ciliary nerves and discovered that it is richly inverted with nerve structures penetrating 360˚ around the circumference [15]. The nerves lie within the superficial stromal level but penetrate the Bowman's membrane to the epithelium. These nerves are important as they provide the cornea with sensations of touch, pain and temperature. Trauma to these nerves can result in chronic neuropathic conditions [16].

1.1.3 The Corneal Epithelium

The corneal epithelium is the outermost layer of the cornea [17]. This layer is composed of approximately five uniform layers of non-keratinised stratified squamous epithelia, supported by a single basal layer of cells [Figure 3][18]. This forms a dynamic barrier against microbes which can cause inflammatory disease. The corneal epithelial cells are linked together by desmosomes, which are intracellular adhesive junctions. These junctions are made up of the transmembrane glycoproteins desmogleins, desmocollins and cytoplasmic plaques plakoglobin and desmoplakin [19].

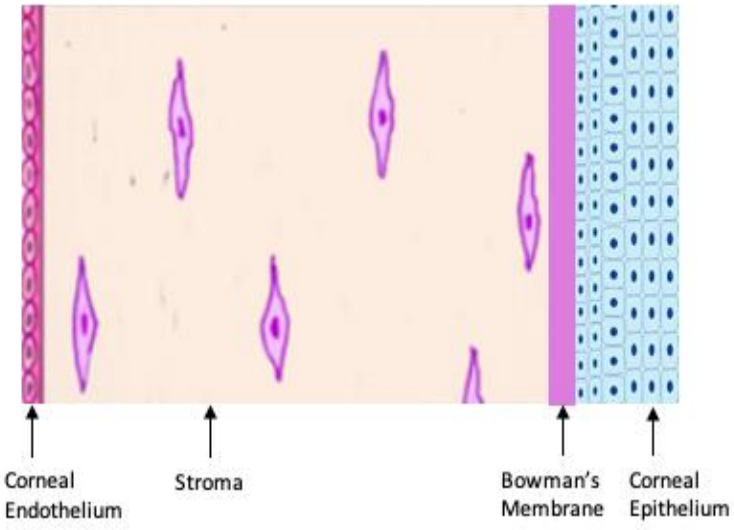

Figure 3: Schematic of the corneal epithelium. The corneal epithelium acts as a barrier to protect the cornea. It is approximately 53 µm deep and constitutes approximately 10% of corneal thickness.

The deepest layer of the corneal epithelium is the basal layer. The basal cells are responsible for the organisation of hemidesmosome complexes to maintain attachment to the underlying basement membrane. This attachment prevents the epithelium from separating from its underlying layers [20].

The basement membrane is made up of highly abundant laminins. The lamina lucida and lamina fibroreticularis establish a portion of the basement membrane, consisting of a collagenous matrix that binds to Bowman's membrane and thus to the rest of the cornea [21]. Bowman's membrane is a non-regenerating layer made up of collagen fibrils. It is located between the epithelial basement membrane and the anterior corneal stroma.

The exact function of Bowman's membrane remains to be elucidated and appears to have no critical function in corneal physiology. It has been suggested that the layer may act as a protective barrier to prevent direct ocular injury with the corneal stroma, hence it is predominately responsible for stromal wound healing [22],[23]. In comparison, the epithelium basement membrane is responsible for anchoring adjacent cells and providing scaffolding during embryonic development [20]. The basement membrane also acts as a semi permeable membrane that determines which substances can enter the epithelium [20].

1.1.4 The Corneal Stroma

The stroma forms approximately 90% of the corneas bulk thickness [21] and is derived embryologically from the cranial neural crest lineage, a source of mesenchymal tissue which also develop the epithelium and endothelium. The corneal stroma is mainly composed of collagen fibres and proteoglycans. These highly organised fibrils not only contribute to the overall integrity of the cornea, but the size and precise arrangement of the stromal fibres and extracellular matrix creates a uniquely transparent tissue [24]. Predominantly within the cornea, collagen type I fibrils can be found, however smaller amounts of collagens type II, IV, VI, XII, XIV and XVIII are also present [25]. New collagens have been discovered and some of these are found within the stroma such as Type VI and Type XIII [24]. This unique homogenous distribution of small collagen fibrils (25 – 30 μm) is likely to be the reasoning behind the production and maintenance of stromal transparency [26].

The collagen type I fibrils are arranged into sheets of lamellar. There are approximately 300 (central cornea) to 500 (limbus) lamellae which comprise the human cornea [1]. These lamellae run parallel to the corneal surface and each layer is arranged into angles relative to fibres in adjacent lamellae. The lamellae extend across the entire length of the cornea without termination.

1.2 The Limbus

The corneal stem cell population can be located within the limbus [27]. The limbal region forms the border between the opaque sclera and the transparent cornea. Regardless of the limbus' small size, it is fundamental to maintain the nourishment of the peripheral cornea. The limbus also includes the

pathway of aqueous humour outflow and is the location for astigmatic keratotomy eye surgery [26]. The limbus' external epithelial cell border between the conjunctiva and cornea possesses multipotent cells for differentiation of various cell types.

1.2.1 Corneal Diseases

Corneal blindness accounts for a significant proportion of blindness globally. The World Health Organisation has estimated that there are approximately 36 million blind individuals worldwide with 1.5 million new cases annually [28] with 4 million of these people suffering from corneal blindness. In the United Kingdom, more than two million people suffer from sight loss which is significant enough to have an impact on their daily lifestyle, such as not being able to drive. The National Eye Health 2016 report states that by 2030, over 2.7 million people in the UK will be visually impaired costing the NHS approximately £3 billion [29]. Figures from the global survey of corneal transplantation show that the number of patients who are in need of corneal transplants have dramatically risen, and at present time only 1 in 70 cases are treated [21]. It should also be noted that approximately 80% of all visual impairment has the potential to be avoided or cured [30]. These figures clearly demonstrate that more can be done to improve sight on a global scale, and that there is clinical need to improve current technologies. The cornea can also be exposed to various genetic and environmental factors which can cause blindness, including:

Nutritional

- Vitamin A deficiency (xerophthalmia)

Infectious

- Fungal keratitis; Bacterial keratitis; Viral keratitis; Trachoma

Degenerative

- Keratoconus

Inflammatory

- Steven's Johnson Syndrome; Mooren's ulcer

Trauma

- Corneal abrasion; penetrating or mechanical trauma from contact lens wear and injuries incurred during surgeries; chemical injury; thermal burns.

1.2.2 Corneal Transplantation and Treatment Procedures

Globally, corneal dystrophies are recognised as the second most common cause of blindness after cataracts. There are surgical procedures available where corneal transplantations can be used for treatment, however there is an international shortage of donor corneas. In third world countries there are also restricted facilities for hospitals and eye banks to produce corneas [31]. Corneal transplantation can restore vision for the majority of those who undergo surgery, with a five-year graft survival rate of 74%. Despite this, statistics have shown that at least one in six full thickness transplants will encounter rejection. The predominant reason behind rejection of the corneas is due to the variation of quality in the donor tissue's epithelial or endothelial health. Patients which have also encountered alkali burns or repetitive graft failures unfortunately have reduced chances of transplantation success [21].

The degeneration of the corneal epithelium can cause visual impairment and blindness through chronic inflammation, scarring and corneal ulceration [32]. Despite limbal stem cells having the capacity to rapidly regenerate the corneal epithelium, if the limbal stem cells have also been destroyed, re-epithelisation is prevented [33]. Restoration of vision is only possible with the re-establishment of epithelial integrity once the cause has been identified and eliminated. As the limbus is the source of cells responsible for epithelial regeneration, corneal repair can be achieved via transplantation of progenitor sources either by a limbal autograft [34] from the contralateral eye, or an allograft. The transplanted tissue is then able to expand *in vivo* to regenerate the corneal surface.

Unfortunately, both treatment options have distinct problems; autologous transplant is only possible in unilateral disease and risks the remaining and likely functional eye to the inherent complications associated with surgery [35]. Allografts on the other hand must first be MHC matched [36], but these still carry the risk of rejection and require life-long immunosuppression. Living-related limbal allografts carry the same risk to the donor as outlined for autografts, whilst still associated with allogeneic complications for the host. However, living-related allografts endure longer than cadaveric allografts. Most allografts eventually fail often lasting no longer than four-five years [37]. It has been reported that if stabilised, using an allograft, host cells can eventually re-populate the cornea despite the absence of donor cell after the critical five-year period. It is also suggested that inadequate immunosuppression may contribute to graft failure [38]. These current issues with shortage of donor corneas and chances of rejection stipulate that there is a high demand for the development of novel therapies that can be used to treat corneal dystrophies globally [21].

1.3 Stem Cells and Cell Therapies

Stem cells are essential for the development of the human body. Stem cells are characterised as specialised cells located in multicellular organisms which can give rise to differentiated cells [39]. These stem cells are characterised by their phenotype (self-renewing properties) through mitotic cell division and differentiation into a range of specialised cells. Stem cells are required for the generation, homeostasis and repair of all cellular components and their self-renewing abilities have immense potential for current and future therapeutic uses in clinic and tissue engineering [40].

Stem cells are subdivided based on their lineage of differentiation [Figure 4] Due to the nomenclature of the stem cells continuously overlapping, there can often be misinterpretation of where the cell derives from [41]. BM-MSCs have been a widely used definition, however Mesenchymal Stem Cells and Haematopoietic Stem Cells can both be extracted from bone marrow. Stem cells may also be defined by their ability to generate different types of cells, for example: HSCs are multipotent, Embryonic Stem Cells are pluripotent, and Limbal Stem Cells (at the conjunctival/corneal boundary) are unipotent [Figure 4E] [42].

The stem cells used in this project are corneal stromal mesenchymal stem cells. These are primary human cells isolated from the stroma of corneal-scleral rims. These cells have the potential to shift to a mesenchymal stem cell phenotype when cultured under the correct conditions.

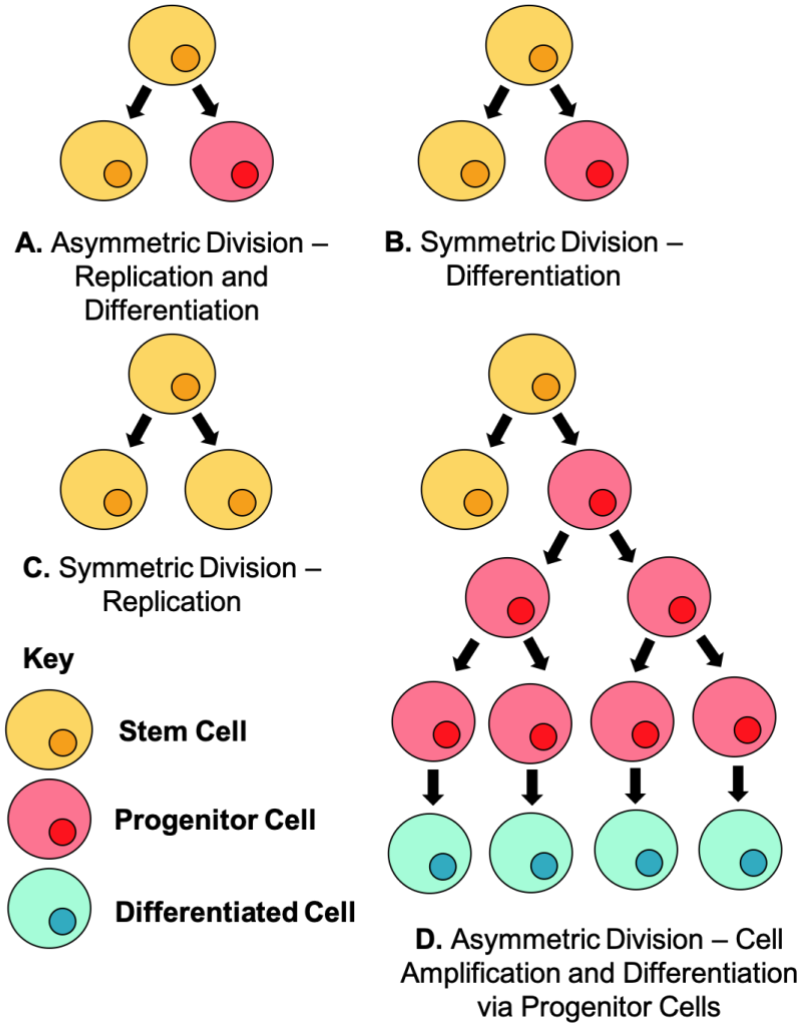

Figure 4: The stages of differentiation. A schematic diagram demonstrating the progression of a stem cell into a terminally differentiated cell. Stem cells play an important role in the body as they give rise to differentiated cells, allowing cell growth by proliferation. **Figure A** represents stem cell self-renewal by asymmetric division, replication and differentiation. One stem cell gives rise to two daughter cells and one of the cells remains identical to itself whilst the other cell differentiates further. **Figure B** and **C** represent systemic division. This is when one stem cell has the potential to give rise to two differentiating cells or two differentiating cells, or an additional two stem cells. **Figure D** represents how transit amplifying cells and progenitor cells are generated. Progenitor cells under-go multiple cycles of cell division to create more cells. After each division, progenitor cells can become more differentiation and thus stop dividing as it has gained characteristics of a differentiated cell type.

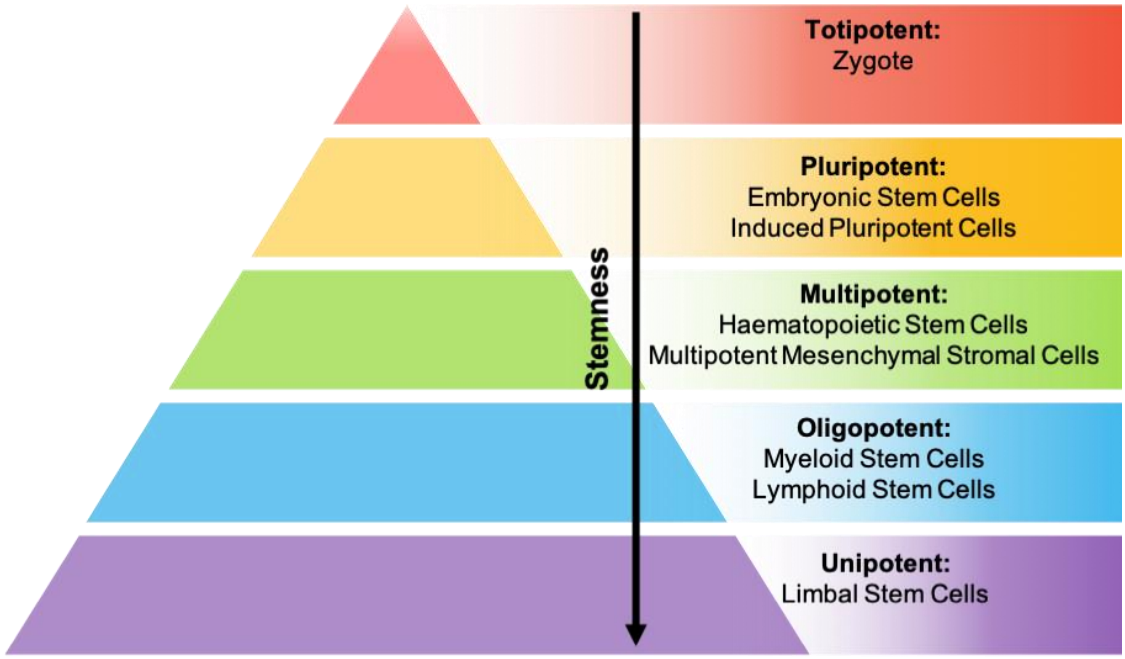

Figure 4E: Hierarchy of stem cells with decreasing potency and self-renewal capacity from top to bottom. As well as potency, stem cells can broadly be divided into adult (yellow, green, blue) and non-adult (red, orange) stem cells. The green and blue sections represent adult stem cells.

The cell therapy industry has a large spectrum of successful therapies which range from regular organ transplants to advanced stem cell therapies [43], [44]. These therapies have been identified in organ transplantation, bone marrow transplantation and blood transfusion. The potential of cell therapy production is growing and clinical targets include diabetes, neurodegenerative disorders, heart disease, spinal cord injury and musculoskeletal disorders.

The industry is currently worth over $8 billion and is expected to be worth over $12 billion by 2020 [45], [43]. Blood transfusions and bone marrow transplants have been previously recognised with high success rates; however, these therapies were developed before the existence of the cell therapy industry. It is becoming increasingly difficult for cell therapies to progress to market. Many therapies must first be approved by the European Medicines Agency (EMA). Regulatory Approval is not the only obstacle when it comes to getting a cell therapy to market. The therapy must first prove effective and improve upon existing medical techniques. Stem cell research is therefore important to aid the understanding of cell behaviour in different environmental conditions, and how control of cell behaviour can be integrated into a therapy as either a success or failure of future cellular based products.

1.3.1 Pluripotent Stem Cells

Pluripotent stem cells possess self-renewing characteristics by diving and developing into the three germ cell layers of the early embryo. The undivided zygote is totipotent and is able to produce all cell types including those that form the extra-embryonic tissues [46]. By the time the zygote has developed into a blastocyst, the inner cell mass also known as embryonic stem cells are pluripotent, capable of forming all the cellular components of the body, but not embryonic tissues such as the placenta [47]. Human embryos for embryonic stem cell research can be isolated from unused cells donated for fertility treatment [48]. Public perception of the ethical and moral issue of human embryonic stem cells manifested through government legislation, currently restricts funding and research on these cells in many countries.

1.3.2 Induced Pluripotent Stem Cells

Induced pluripotent stem cells (iPSCs) are derived from blood or from skin cells which are able to transform back to an embryonic-like pluripotent state enhancing the growth and development of an unlimited source of any human cell required for cellular therapy [49]. iPSCs are transfected *in vitro* and the advance of these cells has gained a lot of attention in the field of tissue engineering and stem cell research [50]. Despite lack of ethical controversy involving iPSCs, there are still limitations and concerns regarding their use, particularly in the utilisation of transection systems and genes required to reprogram cells [51].

1.3.3 Multipotent Stem Cells

Multipotent stem cells include the haematopoietic and mesenchymal stem cells. Despite their reduced stem cell capacity compared to pluripotent stem cells, multipotent stem cells have various advantages [52]. The main advantage of multipotent cells is that they can be harvested from adult sources. This reduces several barriers to their use in a clinical setting. Multipotent stem cells can be given ethically (with informed consent), the potential supply is almost unlimited and autologous or living-related donor transplantations are possible, significantly reducing the chances of immune rejection [53]. Multipotent stem cells offer the greatest stem cell potential available from non-embryonic sources and may therefore represent the greatest potential for cell therapies [54]. These cells are more committed than embryonic stem cells, reducing the complexity of the differentiation process and unwanted cell types and may therefore possess less tumorigenic propensities. The ability of stem cells to self-renew and generate multiple cell types has significant therapeutic potential [42]. In this project, the multipotent stem cells – specifically CS-MSCs will be used.

1.3.4 Mesenchymal Stem Cells

The MSCs are multipotent adult cells which are characterised by a fibroblast-like morphology [55]. The most characteristic feature of MSCs is their capability to differentiate into the three mesenchymal linages: adipocytes, osteoblasts and chondrocytes. In addition, MSCs can also be distinguished by their plastic adherence, and specific cell-marker profile *in vitro* [56]. MSCs have been evaluated for their regenerative applications in maintaining damaged tissues in which they reside. Previous research with MCSs has also shown their potential to influence to immune system and promote neovascularization of ischemic tissues. It was initially discovered in 2002 by Bartholomew et al that MSCs had the ability to modulate immunosuppression of a mixed lymphocyte response *in vitro* and prevention of rejection in a baboon skin allograft model *in vivo* [57].

MSCs additionally secrete immunosuppressive and anti-inflammatory cytokines which interact and mediate lymphocytes associated with the adaptive and innate immune response. MSCs are also able to suppress B cells, T cells, cytokine production and natural killer cells [58],[59],[60],[6]. MSCs can also block the maturation and activation of dendritic cells. Furthermore, MSCs can suppress cells of the MHC identity between the recipient and donor due to their low expression of MHC-II. In the bone marrow, MSCs are known for providing a stromal niche for haematopoietic stem cells [61]. The bone marrow was the primary location where MSCs were identified. They have also been discovered in the adipose tissue, liver, amniotic fluid, umbilical cord, foetal liver blood and bone marrow, kidney, heart, thymus, pancreas and the brain [21].

1.3.5 Keratocytes and Corneal Stromal Stem Cells

The corneal stroma contains a population of cells is conventionally known as keratocytes. Keratocytes are specialised fibroblasts which are neural-crest derived mesenchymal cells [62]. These cells exhibit a dendritic morphology and under regular physiological conditions, keratocytes remain mitotically quiescent; maintaining the highly organised collagen lamellae and proteoglycans mandatory for corneal transparency [63].

At the intracellular level, keratocytes can be identified by molecular markers including crystallin, keratocan aldehyde dehydrogenase, $CD34^-$ and $CD133^+$ [64] If the corneal stroma becomes damaged or diseased, keratocytes either undergo apoptosis or become “activated” in a process which involves TNF-α, TNF-β1, TGF- β2 and IL-1 [64] This activation is accompanied by rapid proliferation and migration to the site of injury and transition into divergent phenotypes. Keratocytes instead acquire myofibroblast scar-forming phenotypes. This transition may be reversible in the long term but is often the cause of scarring and blindness. These repair phenotypes have the potential to either promote

regeneration or induce fibrotic scar formation, resulting in blindness [65]. Previous *in vitro* studies have shown that keratocytes extracted from the limbus display characteristics of the MSCs which conform to a criteria outlined by the International Society for Cellular Therapy and thus keratocytes are of significant interest [66], [67].

It appears that the corneal stroma may contain a heterogeneous mixture of cells with varying stem cell potentials. Keratocytes are isolated from the limbus and peripheral stroma by digesting corneal rims (Manchester Eye Bank) using a collagenase protocol for *ex vivo* culture. Once cells are transferred to tissue culture plastic, they differentiate and alternative cell populations emerge, dependent on the culture environment [25]. The term keratocyte will be reserved only for corneal stromal cells that conform to the keratocyte phenotype [68].

1.4 Good Manufacturing Practice for Cell Therapies

cGMP describes the minimum standard that a pharmaceutical or medical manufacturer must meet in their production process to assure their products are consistently high in quality from batch to batch [69]**.** The cell therapy industry is rapidly developing and becoming an important sector of global healthcare, providing patients with life changing cell therapies [44]. There are currently more than 500 different cell-therapy based companies around the world, however, only a small proportion of these cell therapy products have made it to the cell therapy market, with the majority still in pre-clinical and early clinical development [70]. Medical products that are to be used for regenerative medicine within the United Kingdom (as part of the European Union) must follow specific European Regulations in order to produce pharmaceutical and medical products [71]. GMP regulations have been previously used for the production of vaccines, proteins and monoclonal antibodies [72]. The European Commission decided that in 2004, the tissues and cells directive would re-classify somatic cell therapies and tissue engineered therapies as Advanced Therapy Medicinal Products (ATMPs) and ensure their manufacture applied to the same GMP guidelines.

The Medicines and Healthcare Regulatory Agency is primarily responsible for the production of cell therapies to medical GMP grades. They are responsible for issuing authorisations that ensure appropriate distribution of clinically tested medicines to the cell therapy market, or authorise use for clinical trials [73]. In order to manufacture these products, companies must obtain a manufacturing license by their competent authority [73],[71].

Irrespective of the medical or pharmaceutical product that is being produced (or the type of licensing held by the manufacturing facility) the GMP regulations must always be complied with in order to ensure the consistent production of medicines, which are safe and effective for use. Following EU

regulations, ATMPs, which are classified as sterile medicinal products, must be manufactured within a cleanroom facility to eliminate the risk of contamination.

1.4.1 Manufacturing Facility and Clean Room Maintenance

Manufacturers must continuously monitor laboratory facilities and equipment to ensure they are in working order to reduce the risk of defecting the product. This is usually achieved by using an autonomous system to monitor specific parameters [74]. In addition to an autonomous system, manual monitoring is required to make sure problems with the autonomous system can be managed promptly to avoid loss in product quality [74]. Various parameters are additionally monitored to check that all facilities and equipment are operating to correct specifications such as: humidity and room temperatures, room pressures, particle levels, safety cabinets, CO_2 and humidity levels of incubators and temperatures of fridges and freezers [75].

A clean room is a laboratory where microbial contaminant levels are controlled. Normally in a clean laboratory, the airflow can be laminar or turbulent [76]. Laminar flow is most commonly used by manufacturing facilities. It involves a uni-directional, downward flow of clean air. There are some facilities however which use turbulent flow. This is not uni-directional, and instead particles are moved around the facility until they ultimately reach the ground and towards the extracts [76]. Manufacturers who produce cell therapies require the facility to contain HEPA filters. Usually, these are installed in the ceiling with an extract near the floor which ensures that the majority of the facility is always exposed to airflow. Cell therapy manufacturing facilities should also be designed aseptically for example having smooth surfaces which are easy to disinfect.

1.4.2 Chemically Defined Media

Chemically defined media are growth media which enhance the proliferation of *in vitro* culture of human cells, and all chemical components can be identified [77]. Cell culture media used in laboratories are generally supplemented with an animal or human serum FBS and HPL) as a source of nutrients and poorly identified components. The major disadvantage of in cooperating such serums into media include unidentifiable components, batch variability and the risks of disease transmission. There are clear distinguishable differences between serum-free media and chemically defined media. Serum-free media can contain undefined animal-derived products. These could include albumin, growth factors, carrier proteins or hormones [78]. Undefined animal-derived products are also likely to contain complex contaminants.

In comparison, chemically defined media must contain identifiable components with exact concentrations. Chemically defined media must not contain animal-derived products [74]. This is achieved by this supplementing the media with recombinant versions of albumin and growth factors that are derived from *E.coli* or synthetic chemicals. This project aims to follow similar guidelines for the production of media and cell therapies in accordance to cGMP.

1.4.3 Foetal Bovine Serum

FBS is an extremely common serum supplement used for *in vitro* culture of human cells. Production of FBS has been estimated per year on a global scale to exceed 800,000 litres [79]. This is equivalent to the slaughter of more than two million bovine foetuses annually [79],[80]. FBS is generally obtained from bovine foetuses of pregnant cows sent for slaughter [81]. At this time the foetus is approximately at six months of development [82]. Foetal blood is collected under aseptic laboratory conditions via venepuncture or intracardiac puncture [83]. Once the blood has been drawn, it is then allowed to chill and clot; the serum can then be separated from the red blood cells and fibrin-clotted mass by centrifugation. This method allows FBS to be mass produced in bulk volumes and batches of pre-tested serum can be generated and distributed to laboratories for commercial use.

Due to rich growth factors and simplistic production, FBS is renowned as the most “universally applicable cell culture additive for the stimulation and proliferation of biological products” [84]. FBS is implemented in various protocols for the culture of mesenchymal stromal cells [85],[86]. FBS is highly rich in foetal hormones and growth factors that stimulate cellular proliferation and maintenance [87],[88],[89]. The different types of cell culture media can be seen from Table 1 below.

Table 1. The various types of commercially available culture media

Culture media	Description
Xeno-free media	➢ Derived from the same organism. ➢ No recombinant materials from animal DNA sequences. ➢ Can contain processed or unprocessed materials from human sources. ➢ Recombinant materials made from human, plant, bacterial, or yeast DNA sequences. Animal-derived components may have been used as raw materials at the secondary or tertiary level of manufacturing, unless otherwise stated.
Serum-free media	➢ Media does not contain a serum supplement. Some components may be processed from serum, hormones and ➢ platelet lysate. May contain biological products that are not serum, plasma or haemolymph (tissue extracts such as bovine pituitary extract, platelet lysate, growth factors and growth hormones).
Chemically Defined media	➢ The chemical structures are known and can be identified (by their chemical formula). Examples include: small molecules, salts, carbohydrates, amino acids, steroids and fatty acids. Media does not contain proteins, hydrolysates, or other products with complex structures or unknown compositions.

FBS also has multiple disadvantages. Many compounds within FBS are still unknown as they have not been identified. For the majority of identified compounds, their function of cultured cells is still unclear [90]. There are also significant issues with batch variability which makes pre-testing of each batch of FBS a necessity. [80]. High levels of endotoxin contents of FBS have also raised several questions regarding its safety and suitability [91] as it may provoke immunological responses against xenogeneic serum antigens [86]. Another disadvantage of FBS is that it is a potential source of microbial contaminants [92]. Approximately 20 to 50% of commercially available FBS has been estimated to be virally contaminated [91]. Despite bovine spongiform encephalopathy (BSE) not being a current threat, there are dangers of xenogeneic infections which could potentially cross the species barrier and this concern remains [93]. For these reasons, the expansion of CS-MSC in clinical environments should avoid the use of animal sera. Additionally, desired FBS based products that have been applied to successfully cultivate stromal stem cells for pre-clinical applications must be modified and re-evaluated [94].

Aside from scientific and safety issues, the methods for harvesting the blood from foetal calves has raised questions regarding animal welfare [80], [82]. The foetus is most likely exposed to a degree of pain or discomfort which makes the harvest of the foetal blood questionable [95]. Specific measures should be taken into account to minimise the degree of pain animals are exposed to, for example ensuring the calf is unconscious during the cardiac puncture and blood collection [82]. Despite the disadvantages of FBS, it is still widely used in phase I clinical trials, but under the use of regenerative medicine it is highly regulated [90].

1.4.4 Human Platelet Lysate

Human platelet lysate has been used as an alternative supplement for the expansion of CS-MSCs (including bone marrow MSCs) that is currently used across many clinical trials and laboratories [96]. HPL is obtained from platelet rich plasma (PRP), which can be cultivated from pooled buffy coat – derived platelet concentrates of whole blood or from apheresis [94] [Figure 5]. In comparison to thrombin activated platelet relesate in plasma, which has a complex manufacturing process, HPL can be generated from platelet units by a series of simple freeze-thaw procedures [97].

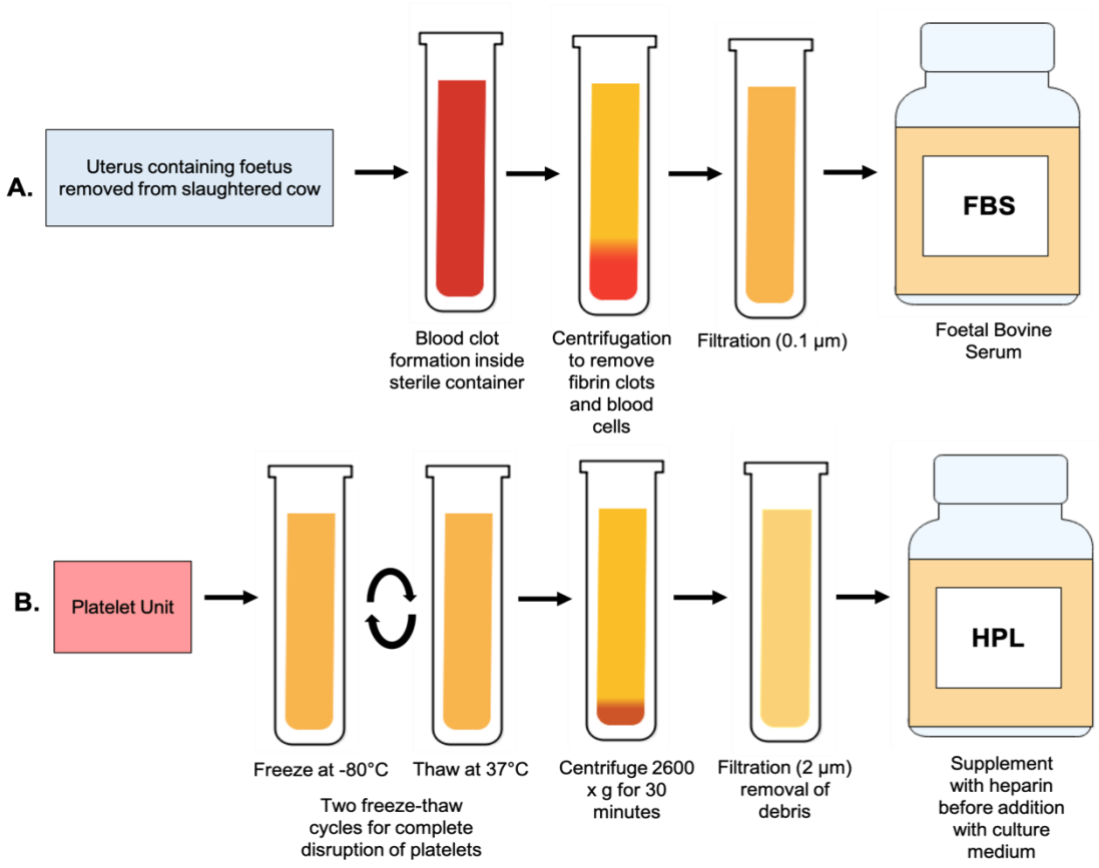

Figure 5: Schematic representing techniques used to generate FBS and HPL. (A) FBS is obtained from the blood of bovine foetuses via cardiac puncture. (B) HPL is generated from platelets via freeze-thaw procedures. The platelet units are aliquoted, frozen down twice at -80˚C, thawed at 37˚C and centrifuged to remove cell debris. The supernatant is filtered and supplemented with heparin to prevent coagulation. Adapted from Hemeda et al 2014 [81].

Poling of the platelet units can further reduce variation between individual platelets. One bag can contain a pool or five harvests of fresh blood, which is combined unless apheresis from individual donors has been performed. Methods have been improved in order to obtain pools of HPL to ensure a balance in batch variation [98], [99]; for example, the pooling of 50 units or more counteracts the variation between individual HPL. Additionally, this provides larger volumes for generation of homogeneous culture media. It is also possible to use autologous HPL to minimise the risk of immunological rejection [99]. The major advantage and difference between FBS and HPL is that HPL can be generated according to cGMP procedures for clinical applications [100], [101].

HPL has numerous advantages and disadvantages when compared to FBS which can be seen in Table II. A significant proportion of studies indicates that HPL assists the culture expansion of CS-MSC at a higher rate than FBS [99]. Additional research has shown that proliferation of adipose tissue derived-MSC is largely increased with the use of HPL [102]. This growth advantage was shown to be less

established using bone marrow derived mesenchymal stem cells (BM-MSC) by Hemeda et al 2014, which suggests that these cell preparations may differ in their nutritional requirements [103]. As HPL is derived from humans, immunological conditions caused by bovine diseases are not a concern [104].

Despite these advantages, HPL also has limitations. Similarly to FBS, HPL is not defined precisely. There are several factors which contribute towards the batch variation of HPL obtained from individual platelet units. Additionally, the use of products which are derived from humans raises ethical concerns which need to be taken into account. Immunological reactions are reduced when HPL is used instead of FBS, but there are still possibilities of a reaction occurring. There are increased disease risks associated with HPL such human immunodeficiency virus (HIV) hepatitis B, hepatitis C, syphilis and human T-lymphotropic virus. All blood products which are collected must receive routine testing for these diseases. In order to further minimise the risk of disease, it is highly recommended to quarantine store the HPL and subject the donor for re-analysis after three months for potential serum conversions [105], [93]. However, such testing and storage is not cost effective in daily research within clinical environments [106].

Table 2. The advantages and disadvantages of FBS and HPL. Green represents FBS and blue represents HPL.

FBS Advantages	FBS Disadvantages
➢ Widely available for many different cell types.	➢ Ingredients are not precisely defined with high batch variation.
➢ Abundantly available (by-product from the slaughter of pregnant cows).	➢ Has the potential to induce immunological reactions against xenogeneic serum antigens.
➢ Available commercially.	➢ Contains a high level of endotoxins.
➢ Previously used in clinical trials with few side effects.	➢ Possible microbial contaminants (prions, bacteria, viruses).
➢ Rich in growth factors.	➢ Animal welfare concerns during cardiac puncture of the bovine foetus.

HPL Advantages	HPL Disadvantages
➢ Can be used for a variety of cell types, particularly for human MSCs, fibroblasts and endothelial cells.	➢ Not precisely defined but human platelets are more standardised than bovine foetal blood.
➢ Rich in growth factors (platelet - derived growth factor).	➢ Variation between individual HPLs.
➢ HPL generated easily by freeze-thaw procedures.	➢ HPL is not available on a commercial scale.
➢ No risks of xenogeneic immune reactions or transmission of bovine related diseases (such as BSE).	➢ Danger of transmitting human diseases such HIV and T-Lymphotropic Virus.
➢ Previously used in clinical trials with low levels of side effects.	

1.5 Thesis Aims and Objectives

This thesis aims to generate an understanding of developing a xeno-free cGMP growth medium for the culture of CS-MSCs with relevance to their potential use as a therapy for corneal regenerative medicine. This will involve *in vitro* analysis of CS-MSCs from different human corneal donors.

The practical objectives by which this will be achieved are as follows:

- Comparison of the use of FBS with HPL to investigate changes in proliferation, morphology and phenotype of the CS-MSCs when cultured in media containing FBS (control group) and HPL (experimental group).
- Comparison of commercial xeno-free media for the culture of CS-MSCs.
- Comparison of the CS-MSCs with BM-MSCs.
- Observe how cell therapies are created by understanding clean room facilities and product packaging and manufacturing at NuVision Biotherapies.

2 Materials and Methods

During this project, a visit was made to the clean room facilities at Nu-Vision Biotherapies, MediCity Nottingham to gain insight into how a regenerative medicine company produces ocular surface therapies according to cGMP.

All cell culture and experimental assays for each donor were carried out as one replicate or more unless otherwise stated.

2.1 Materials

1 x 10^6 viable StemPro™ BM Mesenchymal Stem Cells (A15652) were obtained from ThermoFisher Scientific at P4. StemPro™ BM Mesenchymal Stem Cells were isolated from human bone marrow (donated with informed consent) and expanded under hypoxic (3-5% O_2) conditions. Before cryopreservation at P4, the cells were tested for viability (>90% post-thaw viability), expression of cell surface markers indicative of cell surface markers CD73, CD90, CD105 and their ability to differentiate into osteocytes, adipocytes and chrondrocytes. These tests were peformed by the manufacturer prior to receiving the vial of cells.

Gelatin coating was used to coat all flasks for the xeno-free and BM-MSC experimental procedures due to lack of cell adhesion to the tissue culture plastic. Despite media clearly stating that adhesion was not required for the cells, after vast efforts it was decided that gelatin coating was essential in order to complete the project. Gelatin was used in comparison to Fibronectin as it was inexpensive and readily available with a maximum waiting period of two hours to ensure gelatin had set. Fibronectin unfortunately required an overnight treatment and could not be sourced for the project.

2.2 Media

	Media			
	Type	**Source**	**Xeno-Free**	**Chemically Defined?**
1	PLTMax® Human Platelet Lysate	Merck Millipore	Yes	No
2	StemXVivo	R&D Systems	Yes	No
3	StemPro MSC SFM XF	ThermoFisher	Yes	Yes
4	Mesenchymal XF Expansion	Sigma	Yes	No
5	StemMacs XF	Miltenyi	Yes	No

Table 2.1. Different media used for culturing CS-MSCs including media type, source, Xeno-Free and whether the media is chemically defined.

2.3 Media Sterility

The sterility of cell culture media and chemicals was achieved by use of 0.22 µm filters (ThermoFisher Scientific).

2.4 Tissue

Human corneoscleral rims for research were obtained from Manchester Eye Bank or Nottingham University Hospitals. Human donor tissue was used with approval by the local ethics research committee (NRES Committee East Midlands-Nottingham 1, 07/H0403/140) in accordance with the tenets of the Declaration of Helsinki, following consent from the donors or their relatives. The extracted cells originally expressed a quiescent, keratocyte phenotype, which shifts to a mesenchymal stem cell phenotype by passage 4 (P4) on tissue culture plastic in certain media.

2.4.1 Antibodies

Fluorescently conjugated antibodies used for flow cytometry are listed in Table 2.2. Primary antibodies and fluorescently tagged Alexa-Fluor secondary antibodies used for immunocytochemistry are listed in Table 2.3 and Table 2.4 respectively.

Fluorescently Conjugated Antibodies for Flow Cytometry			
Antigen	**Source**	**Conjugated Alexa-Fluor**	**Dilution**
CD105	ThermoFisher Scientific	PE	1:20
CD90	ThermoFisher Scientific	PE-Cy5	1:20
CD73	ThermoFisher Scientific	PE	1:20
CD34	ThermoFisher Scientific	FITC	1:20

Table 2.2. Conjugated antibodies used for flow cytometry including antigen target, source, conjugated Alexa-Fluor and dilution.

Primary Antibodies for Immunocytochemistry			
Antigen	**Source**	**Species**	**Dilution**
CD105	R&D Systems	Goat	1:200
CD90	Thermo Fisher Scientific	Mouse	1:100
CD73	Thermo Fisher Scientific	Rabbit	1:100
CD34	Sigma Aldrich	Mouse	1:200
α-SMA	LSBio	Mouse	1:200
Vimentin	Vector	Mouse	1:100

Table 2.3. Primary antibodies used for immunocytochemistry including antigen, source, species and dilution factor.

Secondary Antibodies for Immunocytochemistry			
Antibody	**Alexa-Fluor**	**Source**	**Dilution**
Anti-Mouse IgG	488	Invitrogen	1:200
	594	Life Technologies	1:200
Anti-Rabbit IgG	488	Life Technologies	1:200
	546	Life Technologies	1:200
Anti-Goat IgG	546	Invitrogen	1:200

Table 2.4. Secondary antibodies used for immunocytochemistry including Alexa-Fluor, source and dilution factor.

2.4.2 Quantitative reverse transcription polymerase chain reaction (RT-qPCR)

RT-qPCR was used to determine levels of the target gene in the cell samples. Samples were normalized to the relative expression of the house keeping gene *GAPDH*. The probes used can be found in table 2.5 respectively.

Table 2.5. Taquman Probe information.

Gene Name	Protein	Assay ID
ENG	CD105	Hs00923996_m1
THY1	CD90	Hs00174816_m1
NT5E	CD73	Hs01573922_m1
CD34	CD34	Hs500990732_m1
VIM	Vimentin	Hs00185584_m1
ACTA2	α-2-Actin	Hs00426835_g1
GAPDH	GAPDH	Hs99999905_m1

2.4.3 Enzyme-Linked Immunosorbent Assays (ELISAs)

Sandwich ELISAs were used to quantify levels of protein secreted in the cell culture supernatants. Samples were thawed on ice for use on the day of analysis. The proteins tested for can be found in table 2.6 respectively.

Table 2.6. Proteins secreted by CS-MSCs and BM-MSCs as determined by sandwich ELISAs including protein and source.

Protein	Source
IL-1β	R&D Systems
PEDF	R&D Systems
IL-6	R&D Systems
EGF	R&D Systems
HGF	R&D Systems
FGF2	R&D Systems
IL-8	R&D Systems
TGF-1β	R&D Systems

2.5 Methods

2.5.1 Cell Culture

Cell culture was carried out using aseptic technique in a class II microbiological safety cabinet (Envair), fitted with high efficiency particulate air (HEPA) filters. Cell cultures were stored in an incubator (Panasonic Healthcare, Japan) at 37°C in a humidified atmosphere containing 5% CO_2.

2.5.2 Extraction and Isolation of Primary Human CS-MSCs

CS-MSCs are primary human cells isolated from the stroma of corneal-scleral rims. These cells have the potential to shift to a mesenchymal stem cell phenotype by P4 when cultured in certain media.

Stromal cells were isolated from human corneal rims using a collagenase digestion technique, obtaining a single cell suspension through the breakdown of collagen in the extracellular matrix.

Corneal rims were removed from organ culture broth, placed epithelial side down in a petri dish and washed in 1% (v/v) antibiotic-antimycotic (AbAm) in Dulbecco's phosphate buffered saline (PBS). Excess sclera was removed using a scalpel with approximately 1mm left around the limbus for tissue stability. The tissue was divided into approximately 20 small segments and digested in 1mg/ml collagenase type IA (Sigma; G2674).

The tissue was incubated with agitation at 37°C, 5% CO_2, 95% humidity for 5 hours, or until all of the tissue appeared digested. 20% M199 medium (Sigma; M4530) supplemented with 20% (v/v) foetal

bovine serum (FBS) (Sigma; F9665), 2mmol/L L-glutamine (Sigma; G7513), and 1% (v/v) AbAm was added to the digests (1:1) to inhibit the collagenase, and cells were filtered through a 40µm cell strainer to remove remaining undigested tissue. The filtrate was centrifuged at 200g for 4 minutes, the supernatant discarded, and the cell pellet resuspended in 800 µl HPL, consisting of Dulbecco's Modified Eagle's Medium (DMEM/F-12) supplemented with either 10% FBS or 10% PLTMax® Human Platelet Lysate (Merck Millipore; SCM141), 2mmol/L L-glutamine and 1% (v/v) AbAm. Cells were counted using the Countess II FL (Thermo Fisher Scientific) with Trypan blue to calculate a live percentage.

For xeno-free methods, the filtrate was centrifuged at 200g for 4 minutes, the supernatant discarded, and the cell pellet resuspended in 1 ml Stem Cell Medium (SCM), consisting of DMEM/F-12 supplemented with 20% (v/v) Knock Out Serum, (ThermoFisher Scientific; 1082828), 1% (v/v) MEM Non Essential Amino Acids (ThermoFisher Scientific), 4 ng/ml FGF-basic (ThermoFisher Scientific; PHG0026), 5ng/ml Human Leukaemia Inhibitory Factor (Cell Signalling Technologies; 8911SC) and 1% (v/v) AbAm. Cells were cultured in SCM media on gelatin coated T25 flasks until ready for passage. 3,000 cells per cm^2 were collected from each donor in order to ensure that there were enough cells for experimental analysis. The number of cells required to be collected were as follows: 960 cells per 96 well (0.32 cm^2), 28,500 cells per 6 well (9.5 cm^2), 75,000 cells per T25 (25 cm^2) and 225,000 cells per T75 (75 cm^2).

2.5.3 CS-MSC Culture

Prior to cell dissociation, cells were washed once in PBS. For detachment of CS-MSCs from the tissue culture plate into a single cell suspension at each cell passage, cells were incubated in TrypLE Express Dissociation Reagent (Gibco Life Technologies; 10740764) for 10 minutes at 37°C. The single cell suspension was neutralised using HPL or FBS respectively and centrifuged at 250 rpm for 5 minutes for pellet formation. The supernatant was discarded and cells were resuspended in 800 µl HPL. Cell number was measured and calculated using the Countess II FL via Trypan blue uptake, and cells were reseeded at 3000 cells/cm^2. Cells were plated onto T75 flasks with 10 ml of respective media. Cells were incubated at 37°C, 5% CO_2, 95% humidity with full media changed every 3 days. Cells were passaged every 7 days dependent on confluence. Analysis was carried out when cells reached P4.

For the xeno-free cell culture, cells were consistently reseeded at 3,000 cells/cm^2 and were plated onto one gelatin coated T25 flask for each media. At P3, cells were plated onto two gelatin coated T75 flaks per media at 37°C, 5% CO_2, 95% humidity with full media changed every 3 days. Cells were passaged every 7 days dependent on confluence. Analysis was carried out when cells reached P4.

For BM-MSCs, cells were consistently reseeded at 3,000 cells/cm^2 and were plated onto four gelatin coated T75 flasks supplemented with 10% HPL with full media changed every 3 days. Cells were passaged every 7-10 days dependent on confluence. Analysis was carried out when cells reached P6.

2.5.4 Cell Proliferation and Viability

Viable cells are able to maintain a reducing environment within their cytosol. PrestoBlue Cell Viability Reagent (Thermo Fisher Scientific) uses that reducing ability to quantitatively measure cell proliferation and can be used to establish relative viability. Active cells reduce resazurin, a blue compound with no intrinsic fluorescence to resorufin, a red and highly fluorescent compound.

Cell proliferation and viability were assessed by use of PrestoBlue Cell Viability Reagent (Thermo Fisher Scientific). CS-MSCs at P4 were seeded at 960 cells/well in 96-well plates and viability assessed at day 1, 3 and 7 post passage. PrestoBlue solution was diluted 10 fold in the respective cell culture medium. Subsequently, 200 µl of PrestoBlue Cell Viability Reagent was added to each well and incubated for 20 minutes at 37˚C. 100 µl of PrestoBlue solution from each well was then transferred to a clear bottom, black 96-well plate and fluorescence readings were taken on the CLARIOstar® microplate reader (BMG LABTECH) at excitation 535 (25 nm bandwidth) and emission 615 nm (10 nm bandwidth). Gain was initially adjusted depending on the first sample's fluorescence. Measurements were then obtained from the plate reader and data was analysed using GraphPad Prism.

2.5.5 Fluorescent Immunocytochemistry

Immunocytochemistry is a technique in which a specific combination of antibodies and molecules are used to target the location and expression of specific peptides. These antibodies can be labelled to allow visualisation of the protein. In this project, an indirect method of immunocytochemistry was performed, using primary and secondary antibodies.

- **Cell Fixation**

Cell fixation is required to preserve and stabilise cell morphology and to inactivate proteolytic enzymes. Fixation can be achieved using the crosslinking agent formaldehyde.

4% (w/v) formaldehyde was added to samples and incubated for 10 minutes at room temperature. Samples were then washed 3 times with PBS before and after fixation and left submerged in PBS at 4^{o}C.

- **Cell Permeabilization**

Permeabilization of the cells is required to remove cellular membrane lipids and allow for antibodies to penetrate the cells and allow them to reach their target epitope.

Samples were incubated with 0.1% (v/v) Triton X-100 (Sigma, T8787) for 10 minutes at room temperature, with 3 PBS washes before and after.

- **Cell Staining**

Immunocytochemistry uses a specific combination of antibodies and target molecules to detect the expression and location of target peptides. Throughout this project, the indirect immunocytochemistry assay utilised involves the tagging of target cell antigens with primary antibodies, which are subsequently bound to fluorescently labelled secondary antibodies raised against the primary antibody host species. Blocking steps are required to avoid non-specific binding of antibody to Fc receptors. Serum from the secondary antibody host species was used, as it contains antibodies which bind to the non-specific sites, reducing potential background staining.

Samples for immunocytochemistry were cultured on glass bottom chamber slides (Greiner bio-one) and following cell fixation and permeabilization, were incubated for 1 hour in blocking buffer consisting of PBS supplemented with 1% (v/v) bovine serum albumin (BSA; Sigma, A3856), 0.3M glycine (Sigma, G7126), and 3% (v/v) donkey serum (Sigma, D9663). Samples were then incubated overnight at 4^{o}C with primary antibodies (Table 2.1) diluted in wash buffer containing 1% BSA and 0.3M glycine. Samples were incubated with secondary antibodies (Table 2.2) for 1 hour at room temperature. The required samples were subsequently counterstained with Alexa-Fluor 488 phalloidin (Life Technologies, A12379), by incubation for 20 minutes at room temperature. All samples were then counterstained and incubated for 10 minutes at room temp with 0.5 µg/mL 4',6-diamidino-2-phenylindole (DAPI; Life Technologies, D1306). Chamber slides were then mounted in fluorescence mounting medium and samples were imaged at x20 magnification using the Leica (DMIL LED Fluorescence) microscope.

2.5.5.1 Flow Cytometry

Flow cytometry was used for phenotypic analysis, measuring the expression of cell surface and intracellular markers through detection of specifically bound fluorescent antibodies, identified using a series of lasers.

- **Sample Preparation**

CS-MSCs were detached from the flask as previously described, and the cell suspension diluted in ice cold flow buffer, consisting of PBS with 10% (v/v) FBS to reduce cell aggregation non-specific antibody binding, and 0.1% (w/v) sodium azide to prevent the internalisation of the antibody-antigen complex following staining.

- **Cell Surface Staining**

For cell surface staining, 95µl of cell suspension was added to individual flow tubes with 5µl of conjugated antibody as shown in Table 2.3 (PE: CD105, Pe-Cy5: CD90, PE: CD73, FITC: CD34) all obtained from Thermo Fisher Scientific) and incubated at 4^{o}C for 30 min. Additionally, 2 tubes of cells were identically prepared either with no stain or 5µl of PE-Cy5 isotype for controls. Following incubation, 1ml PBS buffer was added to each sample, and the cells were centrifuged at 250g for 5 minutes. Supernatant was aspirated off, and following another wash in 1ml PBS buffer, cells were resuspended in 400µl 4% (v/v) paraformaldehyde (PFA). Samples were left in the solution at 4^{o}C until ready for analysis.

- **Analysis**

10^4 cells per sample were measured using the BD FACSCanto™ II. The isotypes were used as negative controls and the Beckman Coulter Kaluza Analysis Software was utilized to analyse each sample and produce the figures.

2.5.5.2 Microscopy and Imaging

Phase-contrast images were taken on a Leica (DMIL LED Fluorescence microscope) and images were captured with a DFC300 G Camera and LASX imaging software. Images were taken on day 1, 3 and 7 on x10 magnification.

2.5.5.3 RT- qPCR

RT-qPCR is based on polymerase chain reaction (PCR) which enables target DNA to be amplified and quantified. In order to determine the levels of the target genes within each sample, an RLT buffer was applied to lyse samples at P4, and the lysate was homogenized with the use of QIAshredder columns (Qiagen). Total RNA was extracted with the use of an RNeasy mini kit (Qiagen) according to the manufacturer's instructions.

RNA quantity was measured with the use of a NanoDrop spectrophotometer. RNA (1 µg) was transcribed into single-stranded complementary DNA (cDNA) with the use of Superscript III reverse

transcriptase (Life Technologies) with random hexamer primers, according to the manufacturer's instructions. For polymerase chain reactions (PCRs), 1 µl of cDNA was used with inventoried Taqman assays (Applied Biosystems, Life Technologies) (Table 2.4). *GAPHD* was used as a housekeeping gene to determine relative expression levels of genes. Reverse transcription quantitative (RT-q) PCR reactions were analysed by use of the Real-Time PCR Miner algorithm, which calculates efficiency and threshold cycle.

2.5.5.4 Cytotoxicity

LDH Cytotoxicity Assay

Lactate dehydrogenase (LDH) is a soluble cytosolic oxidoreductase enzyme that is released by cells when the plasma membrane is disrupted. The amount of LDH that is released is proportional to the number of lysed cells. The assay works on the principle that LDH present within the sample causes oxidation of lactate to pyruvate, which in turn, catalyses the reduction of NAD+ to NADH. The second step of the reaction uses the NADH to catalyse the conversion of a tetrazolium salt to a coloured formazan product.

The cell culture supernatant media was collected and the release of LDH was analysed by a Pierce LDH Cytotoxicity Assay Kit (Thermo Fisher Scientific) according to the manufacturers' instruction. The absorbance values were then determined by reading the plate at 490 nm and 680 nm using the CLARIOstar® microplate reader (BMG LABTECH).

ToxiLight™ Cytotoxicity Assay

Adenylate Kinase (AK) is present in all cells. A loss of cell integrity, through damage to the plasma membrane, results in the leakage of a number of factors from cells cultured *in vitro* in the surrounding culture medium. The measurement of the release of AK from the cells allows the accurate and sensitive determination of cytotoxicity and cytolysis.

The cell culture supernatant media was collected, and the relative amount of AK was measured using the ToxiLight™ bioassay kit (Lonza) according to the manufacturers' instruction. Emission values were then determined by reading the plate at 555 nm (70-3 nm bandwidth) using the CLARIOstar® microplate reader (BMG LABTECH).

2.5.5.5 Enzyme-Linked Immunosorbent Assays (ELISAs)

A sandwich immunoassay is a method used for the quantification of antigen between two layers of antibodies. Two antibodies are used which bind to different sites on the antigen. The capture antibody

which is highly specific for the antigen is attached to a solid surface. Once the antigen is added, the detection antibody is also added. The detection antibody then blinds the antigen at a different epitope than the capture antibody. As a result, the antigen is 'sandwiched' between the two antibodies. The antibody binding affinity for the antigen is usually the main determinant of immunoassay sensitivity. As the antigen concentration increases, the amount of detection antibody increases which can be measured by colour development.

Secretion of IL-1β, IL-6, IL-8, PEDF (Pigment Epithelium-Derived Factor), EGF (Endothelial Growth Factor), FGF2 (Basic Fibroblast Growth Factor) TGF-1β (Transforming Growth Factor Beta 1) and HGF (Hepatocyte Growth Factor) were analysed by R&D Systems DuoSet® ELISA kits according to the manufacturer's instruction.

2.5.5.6 Statistical Tests

Parametric tests were used in this report as the data was assumed to be normally distributed due to a small sample size and less than five replicates conducted for each experiment. The Two-way ANOVA statistical tests were performed on Presto Blue results and a two-tailed unpaired t-test was used for RT-qPCR results in this report to determine whether results were significant overall. All statistical analysis was performed using GraphPad Prism 7, with statistical significance assumed based on a 95% confidence interval ($P < 0.05$). Levels of statistical significance were symbolised on graphs (where appropriate) with asterisks ($P \leq 0.05$ (*), $P \leq 0.01$ (**), $P \leq 0.001$ (***), $P \leq 0.0001$ (****), NS (Non - Significant)).

3 Results

3.1.1 Culture of CS-MSCs in FBS vs HPL

3.1.2 Morphology of CS-MSCs assessed with phase contrast imaging

Figure 6 and 7 show CS-MSCs cultured in DMEM/F-12 supplemented with 10% FBS for donors 1-5 reached a high level of confluence at day 1 and maintained this confluence to day 7 as shown by phase contrast imaging [figure 6]. CS-MSCs cultured in DMEM/F-12 supplemented with 10% HPL from donors 1-5 attached to the tissue culture plastic at a lower level for day 1 in comparison to attachment level at day 1 for FBS and thus cell proliferation took longer. At day 7, confluence levels for donors 2-5 were similar to that of FBS at day 7. CS-MSCs in FBS were spindle-shaped and aligned as they became

confluent. In HPL, cells had more of a dendritic morphology with multiple processes but became more spindle-shaped and aligned as they became more confluent.

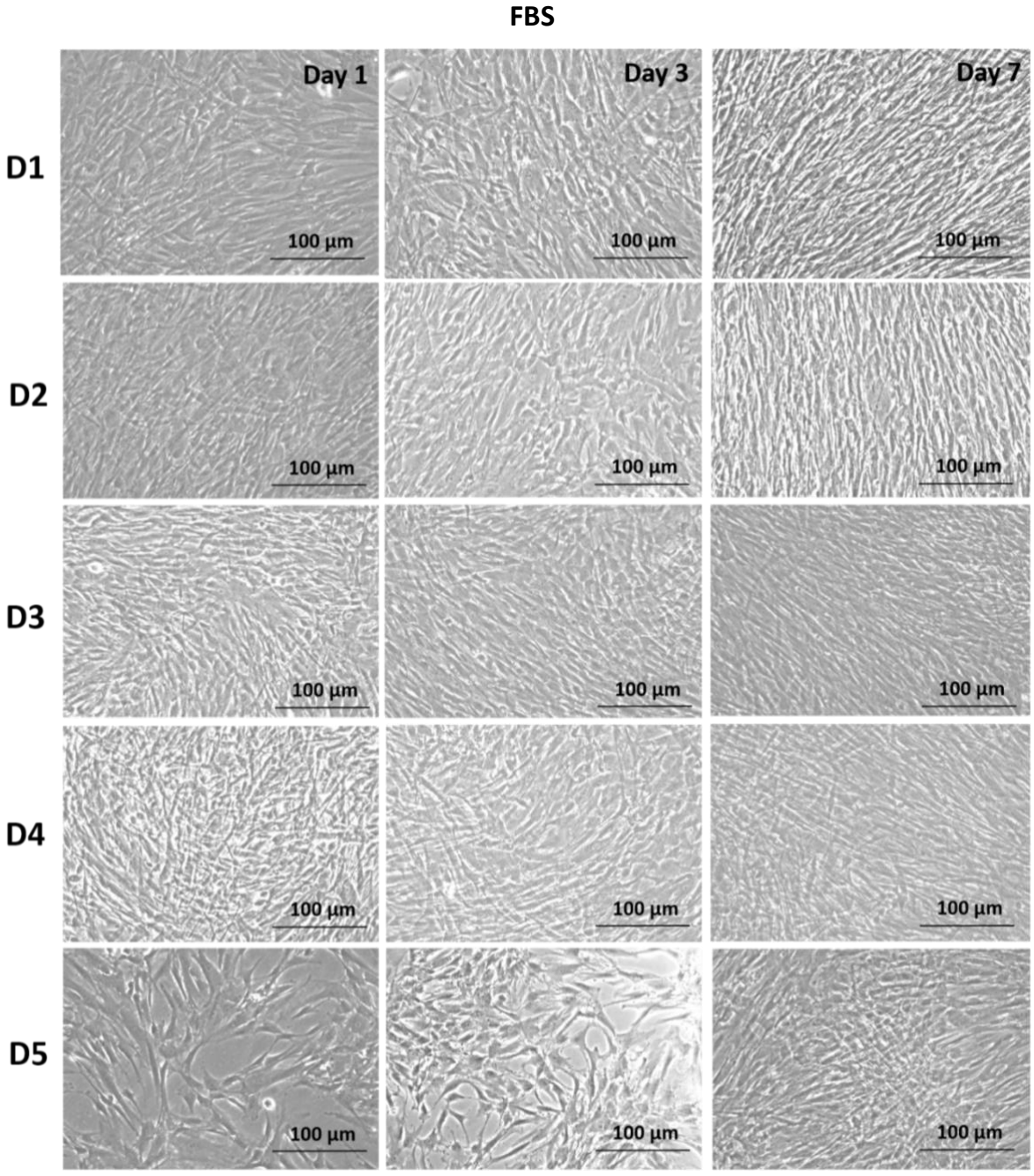

Figure 6. Cell morphology of CS-MSCs. Phase contrast images taken on days 1, 3 and 7 at magnification x10. CS-MSCs derived from five different human corneal-scleral rim donors and cultured in DMEM/F-12 with 10% FBS until P4. Scale bar = 100 µm.

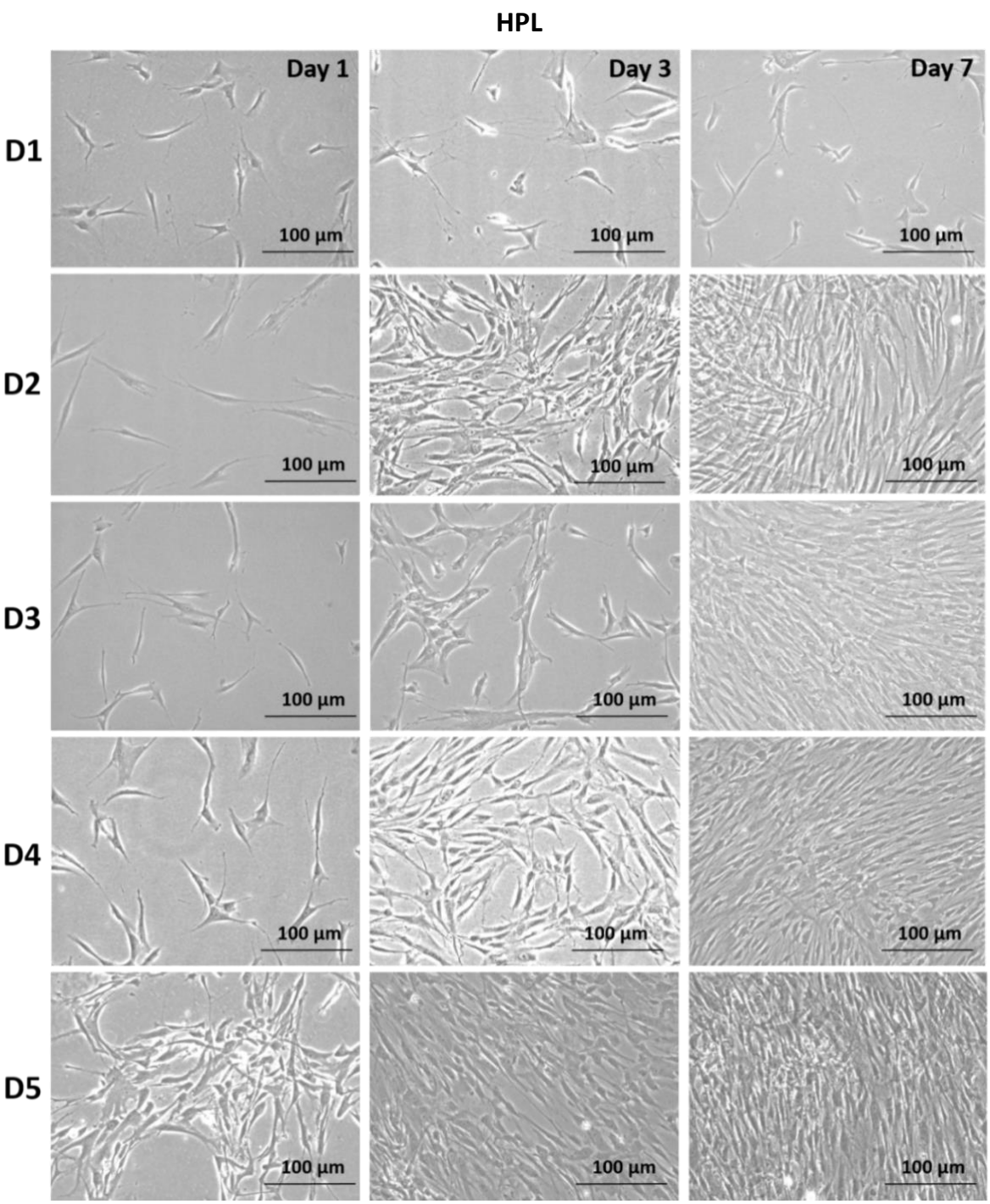

Figure 7. Cell morphology of CS-MSCs. Phase contrast images taken on days 1, 3 and 7 at magnification x10. CS-MSCs derived from five different human corneal-scleral rim donors and cultured in DEMEM/F-12 with 10% HPL until P4. Scale bar = 100 µm.

3.1.3 Cell viability assessment

Figure 8. Cell viability was determined by the Presto Blue assay in 96 well plates. Conversely to the phase contrast images, no significant differences were seen between CS-MSCs cultured in DMEM/F-12 supplemented with 10% FBS and DMEM/F-12 supplemented with 10% HPL. This could possibly be due to the cells in both media reaching confluence by the first time point and thus there being no proliferation over the 7 days.

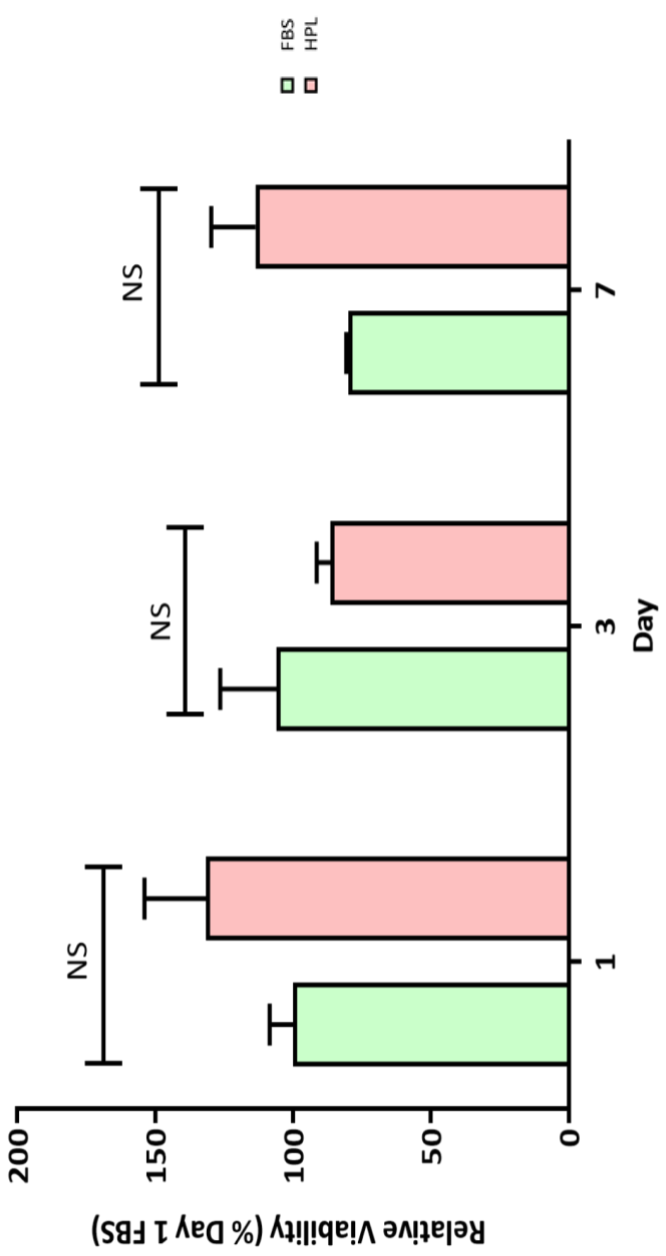

Figure 8. CS-MSCs cultured in FBS and HPL at Days 1, 3 and 7 were subject to analysis using Presto Blue Reagent. The percentage of viable cells relative to Day 1 FBS was calculated. Data are shown as mean ± standard deviation of five different donors (n = 5). Statistical significances comparing FBS and HPL can be seen above. NS = non-significant (two-way ANOVA). Three replicates of this assay were conducted.

3.1.4 CS-MSC marker expression using Flow Cytometry and Immunocytochemistry

Figure 9 and 10. The CS-MSC population for three donors for FBS and HPL were cultured to passage 4 and characterised for the positive MSC markers $CD90^+$, $CD105^+$ and the negative MSC marker $CD34^-$ using flow cytometry [figure 9]. The flow cytometry histograms gave a visual representation of marker expression. $CD90^+$ and $CD105^+$ were constitutively expressed and supported by immunocytochemistry [figure 10] where positive staining was demonstrated for $CD90^+$ and $CD105^+$. $CD34^-$ expression was not seen in flow cytometry in either FBS or HPL, but conversely positive staining was seen during immunocytochemistry in all cells. Additionally, staining for structural analysis of ALDH3A1, Vimentin and actin were also consistent with low levels of the myofibroblast marker α-SMA expressed. 960 cells were seeded per well for staining and expression was maintained across all cell surfaces. Additionally, the keratocyte marker ALDH3A1 which indicates corneal origin did not appear on every cell in FBS and HPL. Vimentin/Actin staining also shows CS-MSC morphology of the cells and indicates CS-MSCs in HPL possess a spindle morphology when compared to CS-MSCs in FBS.

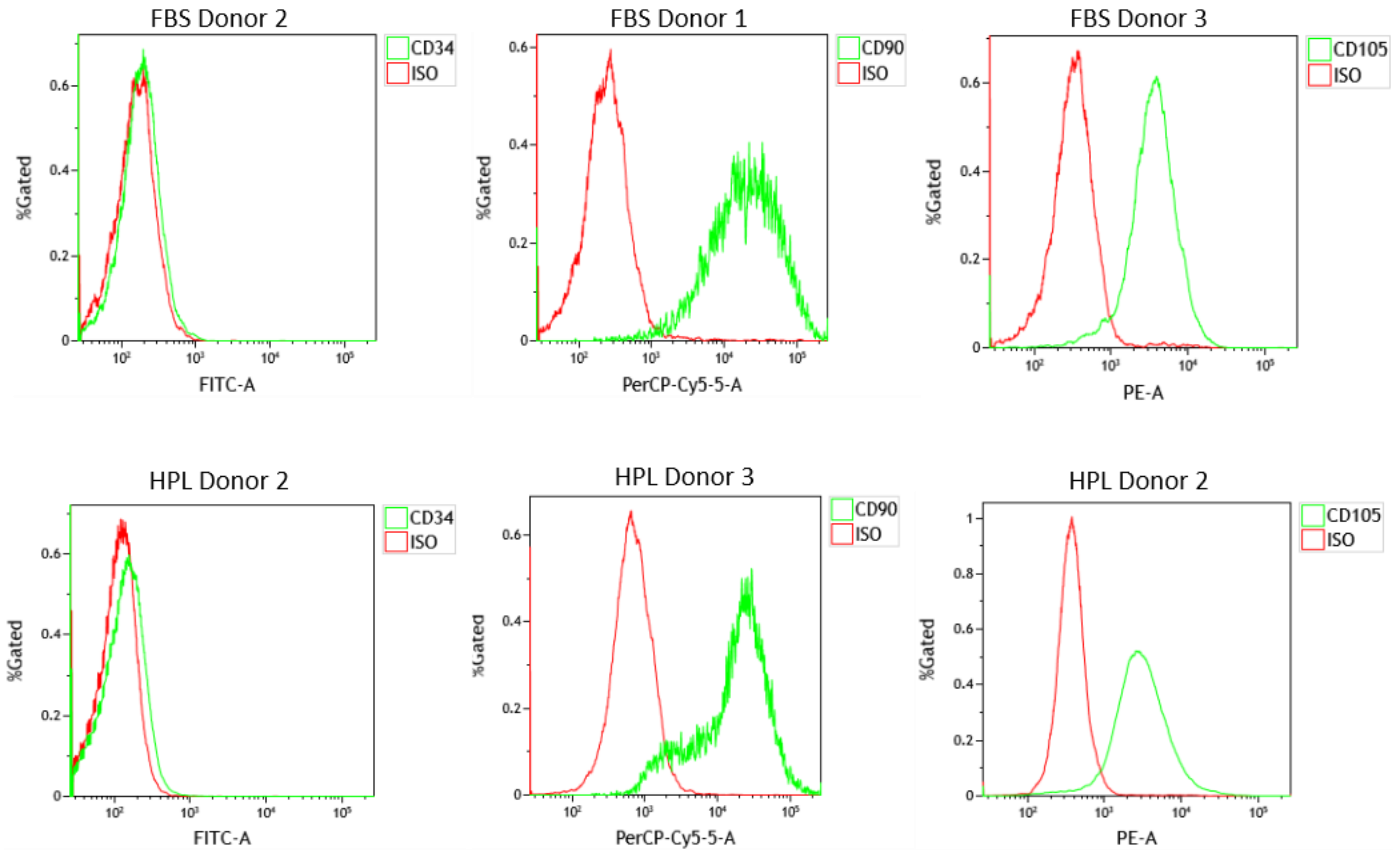

Figure 9. Green lines represent the phenotype of CS-MSCs as determined through cell surface markers $CD34^-$, $CD90^+$ and $CD105^+$ by flow cytometry analysis at P4. Red lines represent the isotype controls.

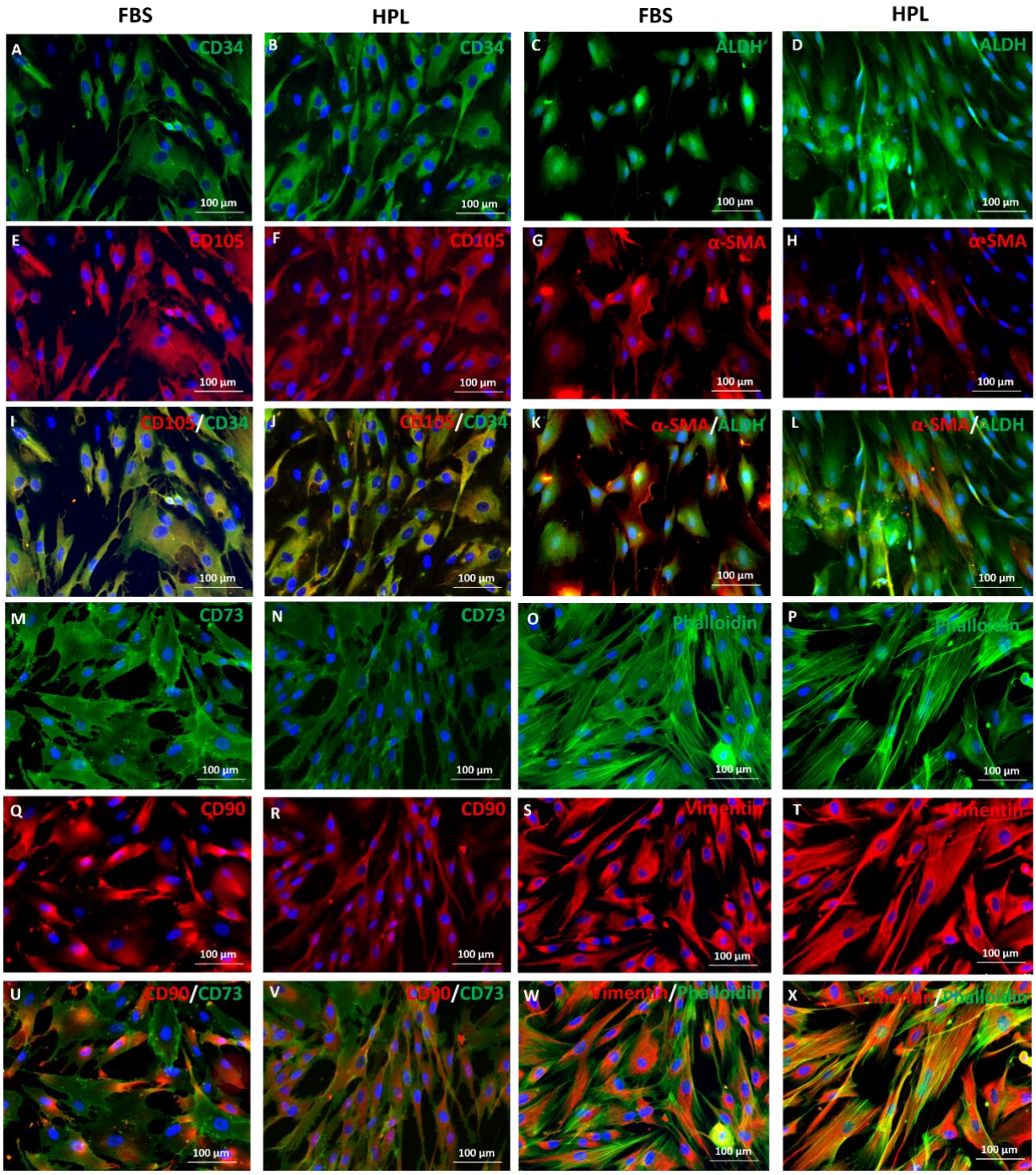

Figure 10. Effect of culture medium on CS-MSC markers from three experimental replicates. Cells were cultured in DMEM/F-12 supplemented with 20 % FBS or HPL. Immunocytochemistry was performed for $CD34^-$ (green), $CD105^+$ (red), $CD90^+$ (red), $CD73^+$ (green), ALDH3A1 (green), α-SMA (red), Vimentin (red) and Phalloidin (green). All images shown with DAPI counterstain (blue); Images taken with fluorescent microscope at x20 magnification. Scale bar = 100 µm.

3.1.5 Percentage Relative Mean Fluorescence Intensity of specific markers

Figure 11. Graphs indicating the percentage relative mean fluorescence intensity of CS-MSCs in FBS vs HPL are shown in figure 11. Levels of the MSC markers $CD90^+$ and $CD105^+$ are consistently expressed in donors 1-3 in FBS and donors 1-4 in HPL, however fluorescence intensity in FBS is approximately 10 times lower than in HPL. The negative CS-MSC marker $CD34^-$ remains at extremely low levels but could be detected. Donors 1-3 for $CD90^+$ and $CD105^+$ FBS showed a range of variation in levels of marker expression but remained consistent for $CD34^-$. There was also a vast level of variation between donors 1-4 for $CD105^+$ for HPL.

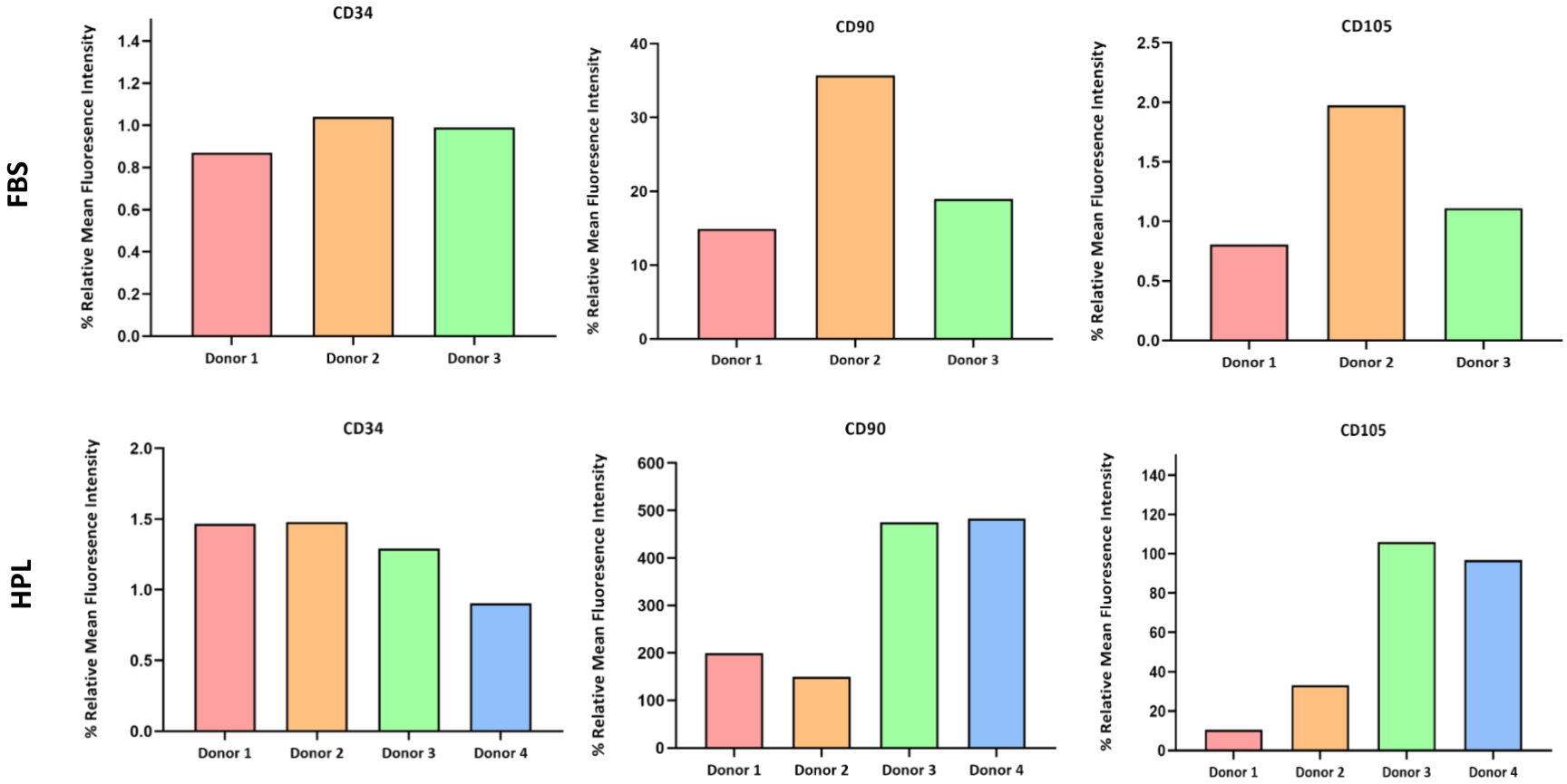

Figure 11. Percentage relative mean fluorescence intensity (rMFI) of CS-MSC markers $CD34^{-}$, $CD90^{+}$ and $CD105^{+}$ in FBS and HPL.

3.1.5.1 Activation of CS-MSCs and quantification of cytokines released by ELISA

Figure 12. To investigate and compare whether CS-MSCs were releasing soluble factors, or if they were using factors present in media only, the CS-MSC culture media of FBS and HPL was collected and compared against media that had not been exposed to the cells. Expression of IL-1β, IL-6, IL-8, FGF-2, TGF-β1, EGF, PEDF and HGF was detected in both CS-MSCs and fresh media although levels secreted varied between the media. Overall, low levels of the pro-inflammatory cytokine IL- 1β was produced by CS-MSCs in both FBS and HPL (HPL = 0.602 pg/mL, FBS = 0.727 pg/mL). Higher levels were present in the fresh HPL media (3.296 pg/mL) indicating that CS-MSCs use IL-1β whereas in FBS fresh media levels of IL-1β (0.374 pg/mL) were low, indicating that CS-MSCs are additionally producing the cytokine.

Secretion of pro-inflammatory IL-6 was extremely high in HPL CS-MSCs (1023.501 pg/mL) in comparison to FBS CS-MSCs (222.463 pg/ml). Very low levels of IL-6 were present in the fresh media (HPL = 5.539 pg/mL, FBS = 3.133 pg/mL) indicating that CS-MSCs were secreting moderate concentrations of IL-6 in HPL. Pro-inflammatory IL-8 was also secreted at high levels in HPL CS-MSCs (1244.784 pg/mL) in comparison to FBS CS-MSCs (222.883 pg/mL) with levels of secretion in the fresh media being relatively low (HPL = 41.522 pg/mL, FBS = 16.108 pg/mL).

FGF-2 was secreted by HPL CS-MSCs at a concentration of (19.736 pg/mL) and a lower level by FBS CS-MSCs (1.630 pg/mL). The fresh media contained a slightly higher level in HPL (26.541 pg/mL) which indicates CS-MSCs were using the growth factor present in the media they were cultured in. Minimal secretion of FGF-2 was present in the FBS fresh media (1.641 pg/mL) indicating that the CS-MSCs were producing the growth factor.

TGF- β1 was secreted in extremely high amounts by HPL CS-MSCs (2921.969 pg/mL). The fresh media also appeared to contain a high level of TGF- β1 (4425.558 pg/mL) which the HPL CS-MSCs appear to have been using. In contrast, FBS fresh media only contained 368.953 pg/mL and the FBS CS-MSCs contained 248.815 pg/mL indicating the CS-MSCs were using up the growth factor.

EGF appeared to be present at high levels in the HPL fresh media (93.166 pg/mL) and HPL CS-MSCs appeared to be using the growth factor (30.639 pg/mL). EGF was additionally present in FBS fresh media at low levels (0.302 pg/mL) with additional production of EGF by FBS CS-MSCs (0.346 pg/mL).

PEDF was present at high levels in the fresh media for HPL (5181.188 pg/mL) with additional production by HPL CS-MSCs (5964.928 pg/mL) Additionally, PEDF was present in FBS fresh media (137.552 pg/mL) with a significant amount produced by the FBS CS-MSCs (4036.547 pg/mL).

HGF present in HPL fresh media was high (178.934 pg/mL) with HPL CS-MSCs secreting (102.441 pg/mL) indicating the CS-MSCs were using the growth factor. The FBS fresh media only contained (28.89 pg/mL) with additional production by FBS CS-MSCs (43.832 pg/mL).

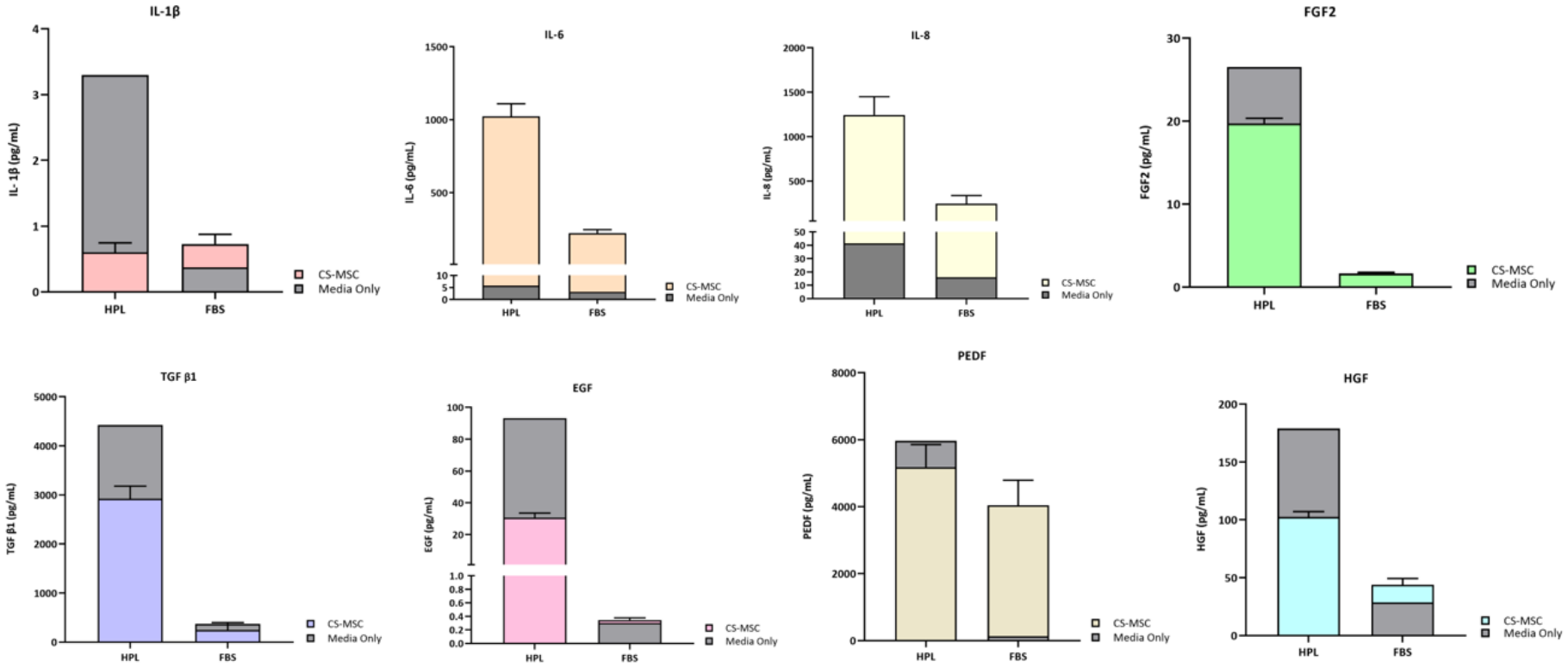

Figure 12. Presence of cytokines and growth factors was determine using Enzyme-Linked Immunosorbent Assay (ELISA) of collected cell supernatant and media. Cytokines tested for: IL-1β, IL-6, IL-8, TGF-β1, EGF, PEDF, HGF and FGF2. Data are shown as mean pg/mL ± standard deviation. One replicate to determine levels of cytokines and growth factors were conducted for this experiment using five donors (*n* = 5).

3.1.5.2 Gene expression in FBS vs HPL using RT-qPCR

Figure 13. RT-qPCR detected no significant differences between levels of gene expression in CS-MSCs cultured in FBS vs HPL for the genes *ENG*, *THY1*, *NT5E*, or *VIM* whereas *ACTA2* expression in HPL was reduced in comparison to FBS. This was proven to be statistically significantly when a two-tailed unpaired t-test was conducted (P = 0.0015). Additionally, there was no gene expression detected for $CD34^-$ in either FBS or HPL, once again conversely to the protein expression detected by immunocytochemistry in figure 10A and figure 10B.

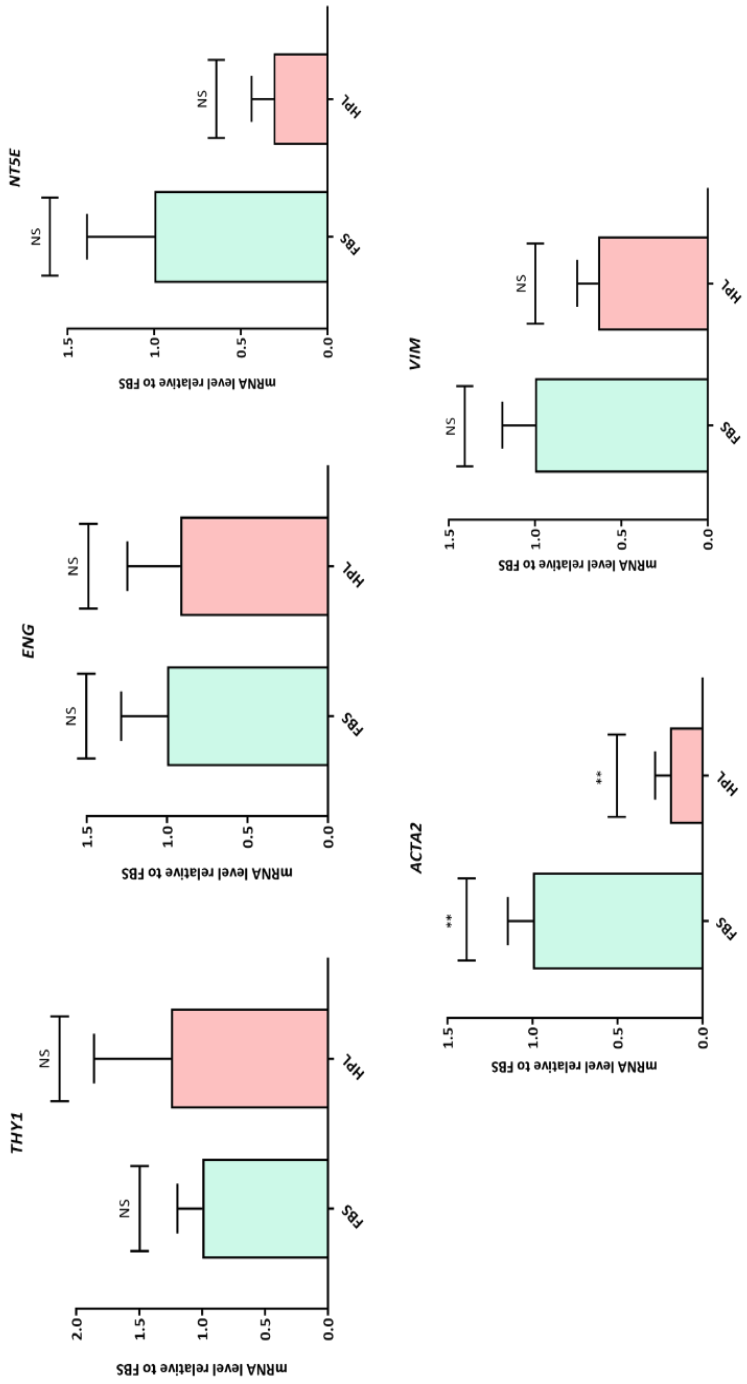

Figure 13. RT-qPCR of CS-MSC expression in FBS vs HPL media with mRNA levels relative to FBS. RT-qPCR was performed for the following genes: *ENG*, *THY1*, *NT5E*, *VIM* and *ACTA2*. Statistically significant values from unpaired t-tests represent (NS = not significant, ** = P ≤ 0.01). Data are shown as mean ± standard deviation. One replicate of RT-qPCR was conducted to determine levels of gene expression of five donors (n =5).

3.2 Culture of CS-MSCs in Xeno Free Media and Chemically Defined Media

3.2.1 Morphology of CS-MSCs assessed with Phase Contrast Imaging

Figure.14. CS-MSCs cultured in various xeno-free and chemically defined media: 1 = PLTMax Human Platelet Lysate, 2 = Stem X Vivo, 3 = StemPro MSC SFM Xeno Free, 4 = Mesenchymal XF, 5 = StemMACS XF. All CS-MSCs were at similar levels of confluence at day 1 and day 3. The CS-MSCs exhibit more of a spindle-like morphology which is a morphological characteristic of MSCs. All CS-MSC morphologies appear to be similar across all media.

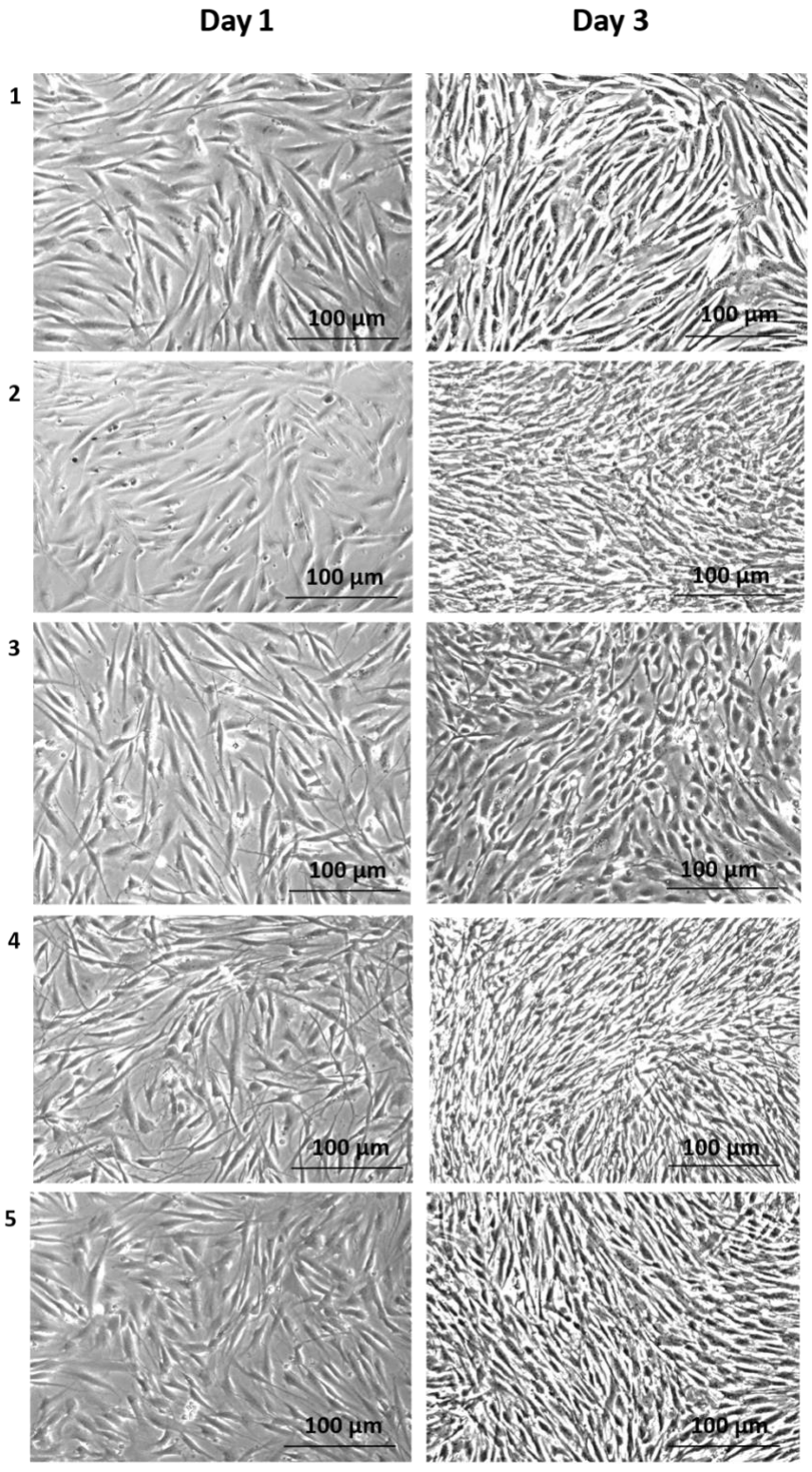

Figure 14. Cell morphology of CS-MSCs in Xeno-Free and Chemically Defined Media at P4 of five different pooled donors. 1 = PLTMax Human Platelet Lysate, 2 = Stem X Vivo, 3 = StemPro MSC SFM Xeno Free, 4 = Mesenchymal XF, 5 = StemMACS XF. Phase Contrast Images taken on Days 1 and 3 at magnification x10. Scale bar = 100 µm.

3.2.2 Cell viability assessment

Figure 15. Presto Blue cell viability assay showing the viability of the CS-MSC in xeno-free and chemically defined media relative to Day 1 HPL. All media appear to support the adherence and initial viability of CS-MSCs at similar levels with Stem X Vivo appearing the most successful.

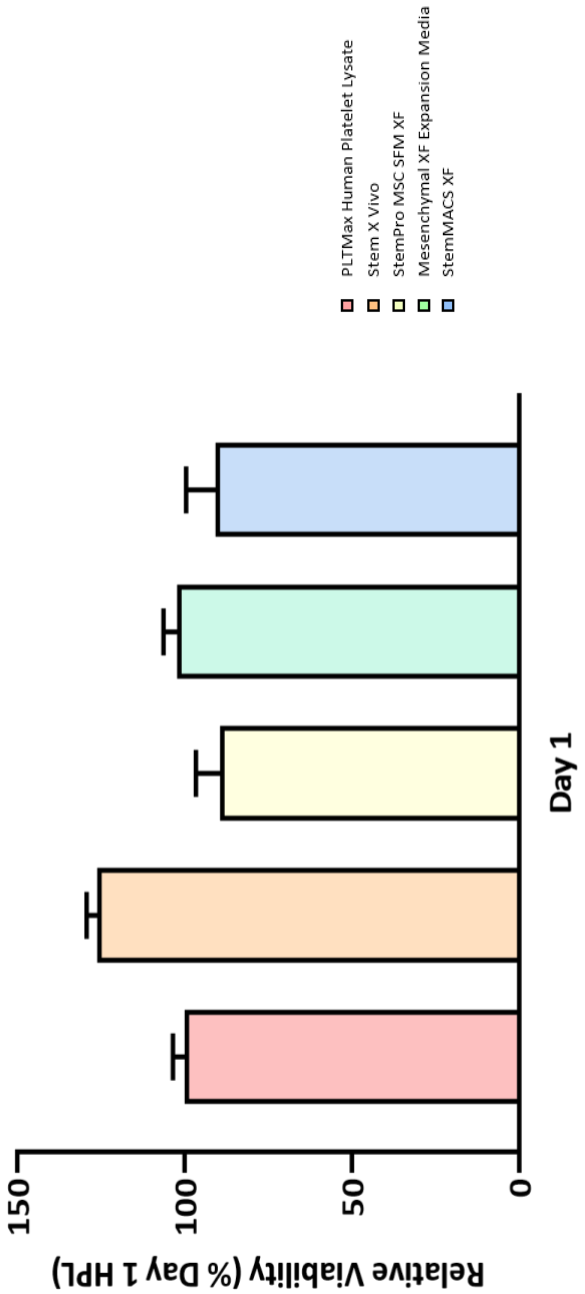

Figure 15. CS-MSCs cultured in xeno-Free and chemically defined media at day 1 were subject to analysis using Presto Blue Reagent. The percentage of viable cells to day 1 HPL was calculated. Data are shown as mean ± standard deviation. Three replicates of Presto Blue were conducted to determine levels of cell viability using five pooled donors.

3.2.3 CS-MSC marker expression using Flow Cytometry and Immunocytochemistry

Figure 16. The CS-MSC population for the xeno-free and chemically defined media were cultured to passage 4 and characterised for the CS-MSC markers $CD73^+$, $CD90^+$, $CD105^+$ and the negative MSC marker $CD34^-$ using flow cytometry. The flow cytometry histograms gave a visual representation of marker expression. **Figure 17.** The CS-MSC markers were expressed at different levels in the media and supported by immunocytochemistry where staining was seen for $CD73^+$, $CD90^+$ and $CD105^+$. $CD34^-$ expression was not seen in flow cytometry in any of the media, but iconversely positive staining was seen during immunocytochemistry in all cells. **Figure 18.** Additionally, staining for structural analysis of ALDH3A1, Vimentin and actin were analysed. HPL [Figure 18.1], StemPro MSC SFM [Figure 18.3] and Mesenchymal XF [Figure 18.4] expressed relatively low levels of α-SMA in comparison to Stem X Vivo [Figure 18.2] and StemMACS XF [Figure 18.5]. CS-MSCs cultured in Stem X Vivo and StemPro MSC SFM expressed more of a spindle like morphology when compared to HPL. Staining appeared across all CS-MSCs in each media. Serum containing media HPL, Stem X Vivo and Mesenchymal XF maintained better MSC morphology than the two serum free media StemPro MSC and StemMACS.

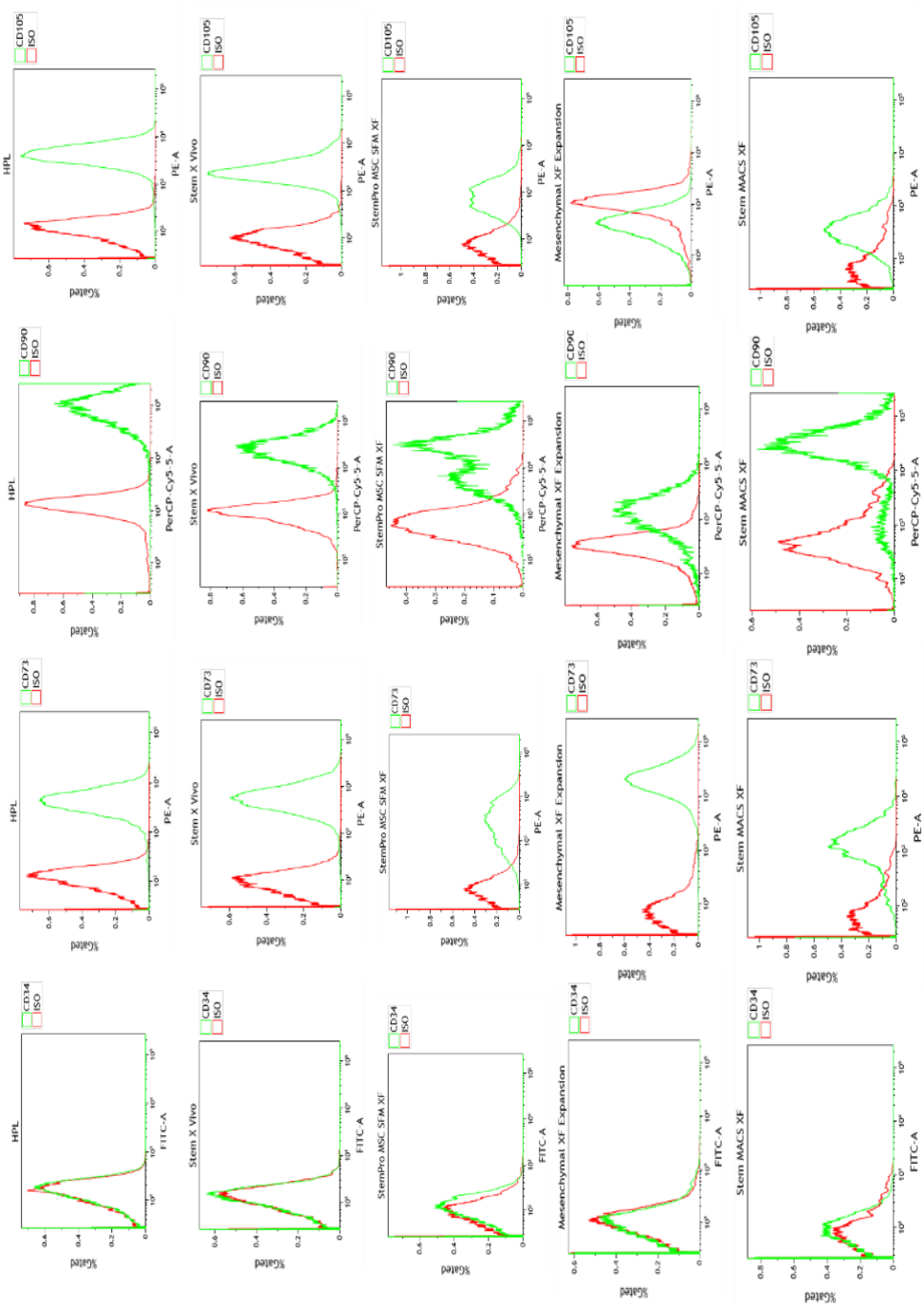

Figure 16. Green lines represent the phenotype of CS-MSCs as determined through cell surface markers $CD34^-$, $CD73^+$, $CD90^+$ and $CD105^+$ by flow cytometric analysis at P4. Red lines represent the isotype controls.

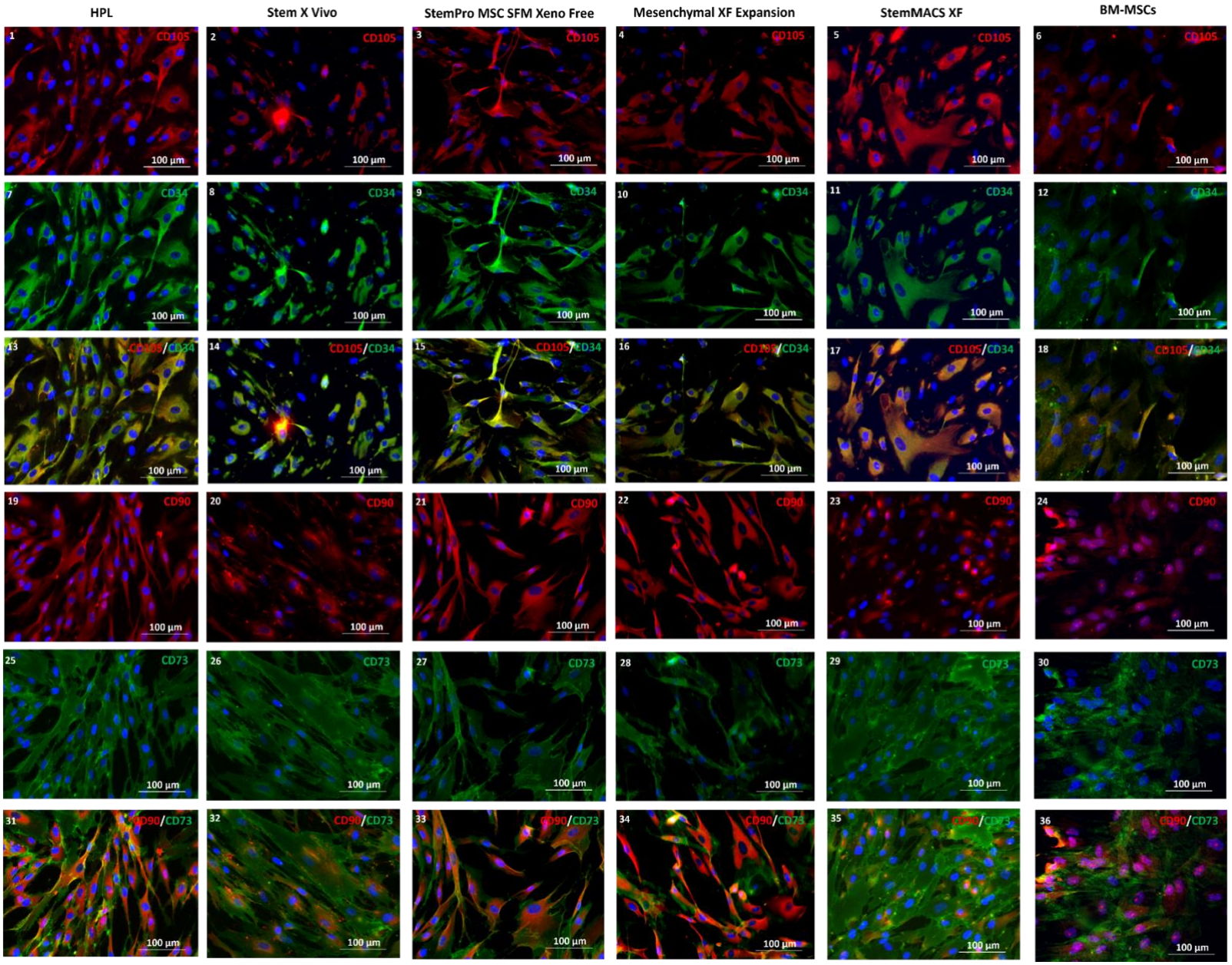

Figure 17. Effect of Xeno-Free/Chemically Defined culture medium on CS-MSC and BM-MSC markers at Day 7 P4. Immunocytochemistry was performed for $CD34^-$ (green), $CD105^+$ (red), $CD90^+$ (red) and $CD73^+$ (green). All images shown with DAPI counterstain (blue); Images taken with fluorescent microscope at x20 magnification. Scale bar = 100 µm.

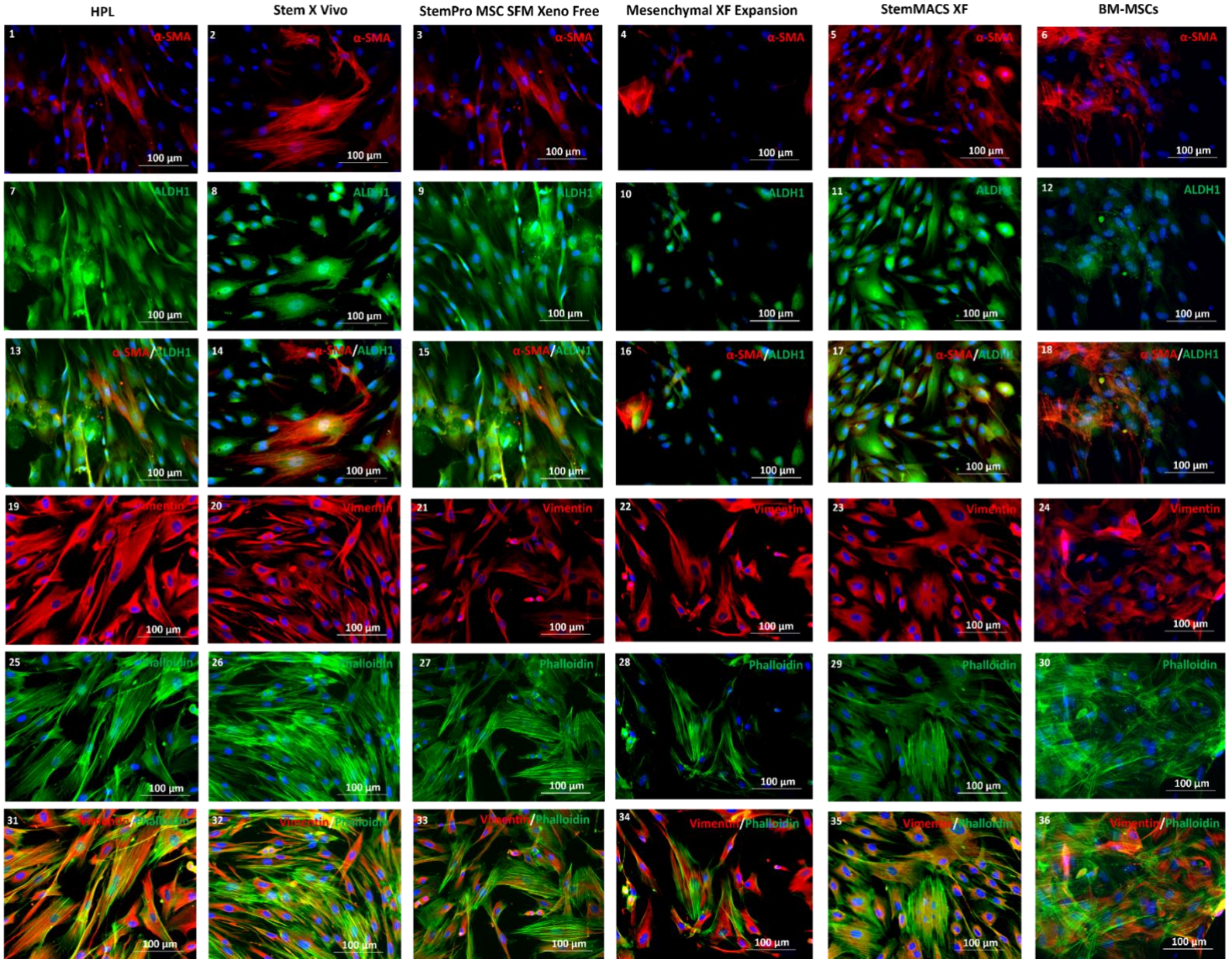

Figure 18. Effect of Xeno-Free/Chemically Defined culture medium on CS-MSC and BM-MSC markers at Day 7 P4. Immunocytochemistry was performed for α-SMA (red), ALDH3A1 (green), Vimentin (red) and Phalloidin (green). All images shown with DAPI counterstain (blue); Images taken with fluorescent microscope at x20 magnification. Scale bar = 100 µm.

3.2.4 Potential Media Cytotoxicity

Figure 19. Any potential cytoxocity caused by the different media was measured by the ToxiLight assay and the LDH assay. All xeno-free media assessed by ToxiLight™ indicated a significantly less cytotoxic effect than when culture in the HPL medium. StemPro MSC SFM XF had the highest emission for toxicity (mean = 72.38%) and Stem X Vivo had the lowest emission for toxicity (mean = 16.27%). Mesenchymal XF and StemMACS XF also had slightly lower levels of toxicity than StemPro MSC SFM XF (mean: Mesenchymal XF = 54.86% and StemMACS = 33.37%). LDH absorbance levels were additionally consistent with ToxiLight™ and were statistically significant. StemPro MSC SFM XF appeared to have the highest level of absorbance (mean = 170.2%) and Stem X Vivo had the lowest level (mean = 26.48%). Mesenchymal XF and StemMACS XF were both relatively low with similar toxicity levels (mean: Mesenchymal XF = 40.59% and StemMACS = 36.48%).

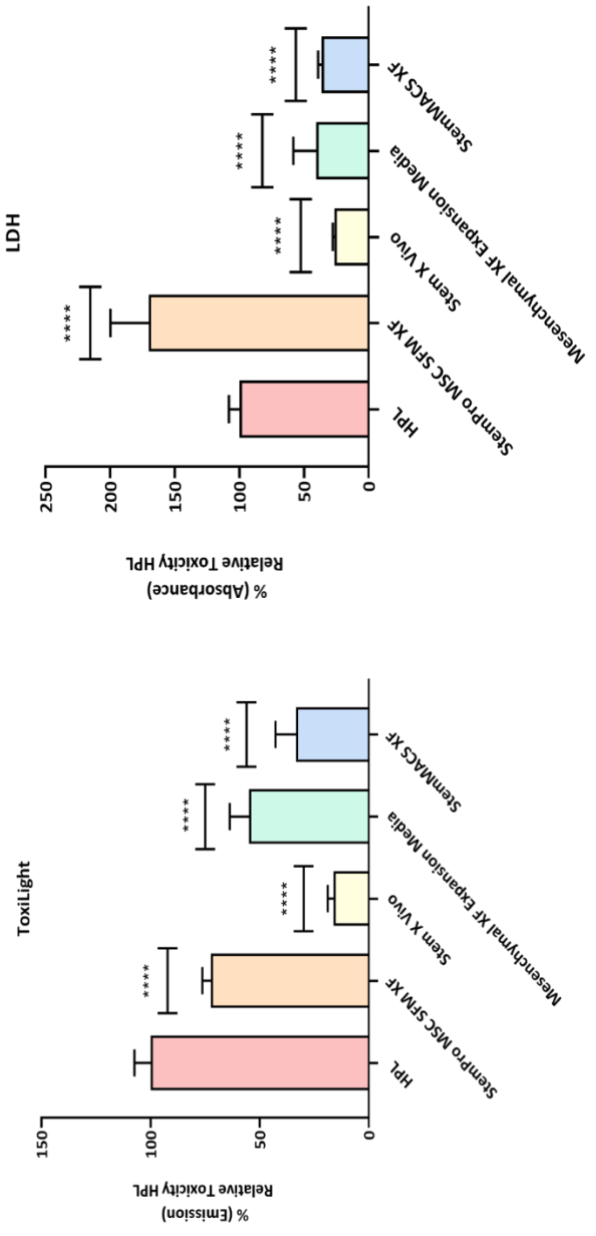

Figure 19. Relative toxicity levels in ToxiLight and LDH assays to the relative toxicity of HPL across five pooled donors. Relative percentage emission for Xeno-free and chemically defined media gave statistically significant values from one way Anova (**** = $P \leq 0.0001$). Data are shown as mean ± standard deviation. Three replicates of LDH were conducted to determine relative toxicity.

3.2.4.1 Activation of CS-MSCs and quantification of cytokines released by ELISA

Figure 20. To investigate and compare whether CS-MSCs were releasing soluble factors, or if they were using factors present in media only, the CS-MSC culture media of HPL, Stem X Vivo, StemPro MSC SFM XF, Mesenchymal Expansion and StemMACS XF were collected and tested as previously described in section 3.1.5.2. Expression of IL-1β, IL-6, IL-8, FGF2, TGF-β1, EGF, PEDF and HGF was detected in both CS-MSCs and fresh media although levels secreted varied between the media. Overall, low levels of the pro-inflammatory cytokine IL- 1β was additionally produced by CS-MSCs in HPL, Stem X Vivo, StemPro MSC SFM XF and Mesenchymal Expansion (mean = 0.6 pg/mL to 1.186 pg/mL). Stem MACS XF however contained significantly higher levels of IL-1β in the fresh media (7.46 pg/mL) indicating CS-MSCs were using the cytokine present in the fresh media.

Secretion of pro-inflammatory IL-6 was relatively high in all five media CS-MSCs were present in (means = 677.588 pg/mL to 1089.090 pg/mL). This indicates that CS-MSCs were secreting moderate concentrations of IL-6 into the media. Pro-inflammatory IL-8 was also secreted at similar levels to IL-6 across all of the media containing CS-MSCs (482.860 pg/mL to 1250.378 pg/mL).

FGF-2 was present in the fresh media of HPL (mean = 541.778 pg/mL), Stem X Vivo (92.24 pg/mL), StemPro MSC SFM XF (227.17 pg/mL). Levels were much lower in Mesenchymal XF (5.559 pg/mL) and StemMACS XF (43.418 pg/mL). CS-MSCs in Mesenchymal XF were additionally producing FGF2 (8.208 pg/mL).

TGF- β1 was secreted at moderate levels by CS-MSCs in HPL (mean = 316.194 pg/mL), Stem X Vivo (mean = 292.179 pg/mL) and StemPro MSC SFM XF (mean = 772.575 pg/mL) in comparison to CS-MSCs in StemMACS XF where additional TGF- β1 was not produced, and levels were higher in the fresh media (mean = 3187.214 pg/mL).

EGF was present in various concentrations in fresh media of HPL (mean = 0.401 pg/mL), StemPro MSC SFM XF (mean =169.375 pg/mL) and StemMACS XF (82.311 pg/mL) indicating CS-MSCs were using the growth factor. Stem X Vivo and Mesenchymal XF in comparison produced additional amounts of EGF (mean: Stem X Vivo = 0.392 pg/mL, Mesenchymal XF = 0.723 pg/mL).

PEDF was additionally produced my CS-MSCs in all media at extremely high levels (mean = 5040.380 pg/mL to 5638.278 pg/mL). Levels of PEDF were very similar in StemMACS XF (mean: fresh media = 5597.268 pg/mL, CS-MSCs = 5638.278 pg/mL).

HGF was also additionally produced by CS-MSCs in all media at various levels (mean: 65.415 pg/mL to 1298.807 pg/mL).

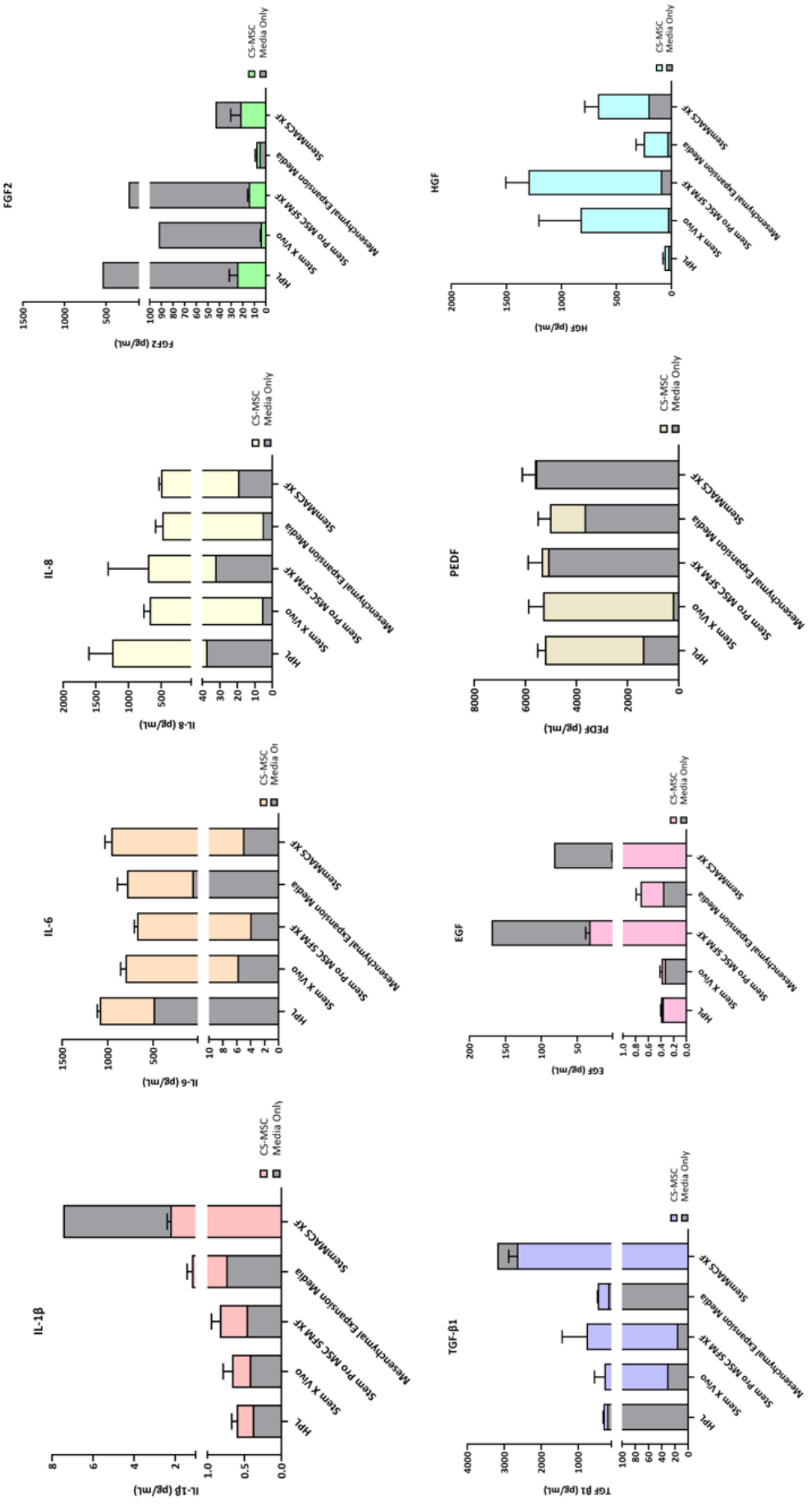

Figure 20. Presence of immunomodulatory cytokines was determined using Enzyme-Linked Immunosorbent Assay (ELISA) in five pooled donors. Cytokines tested for: IL- β, IL-6, IL-8, TGF- β1, EGF, PEDF, HGF, FGF2. One replicate to determine levels of cytokines and growth factors was conducted using ELISA for five pooled donors.

3.2.4.2 Gene expression in Xeno-free and chemically defined media

Figure 21. RT-qPCR detected no significant difference between levels of gene expression in CS-MSCs cultured in xeno-free and chemically defined media for the genes *ENG*, *NT5E* and *ACTA2*. The genes for *THY1* proved to be statistically significant for the mRNA level relative to HPL for Mesenchymal XF (P = 0.01) and *VIM* for the mRNA level relative to HPL for Mesenchymal XF (P = 0.001) and StemMACS XF (P = 0.05). Additionally, there was no gene expression of $CD34^-$ in any of the media which was detected by immunocytochemistry in figure 16 and figure 17.

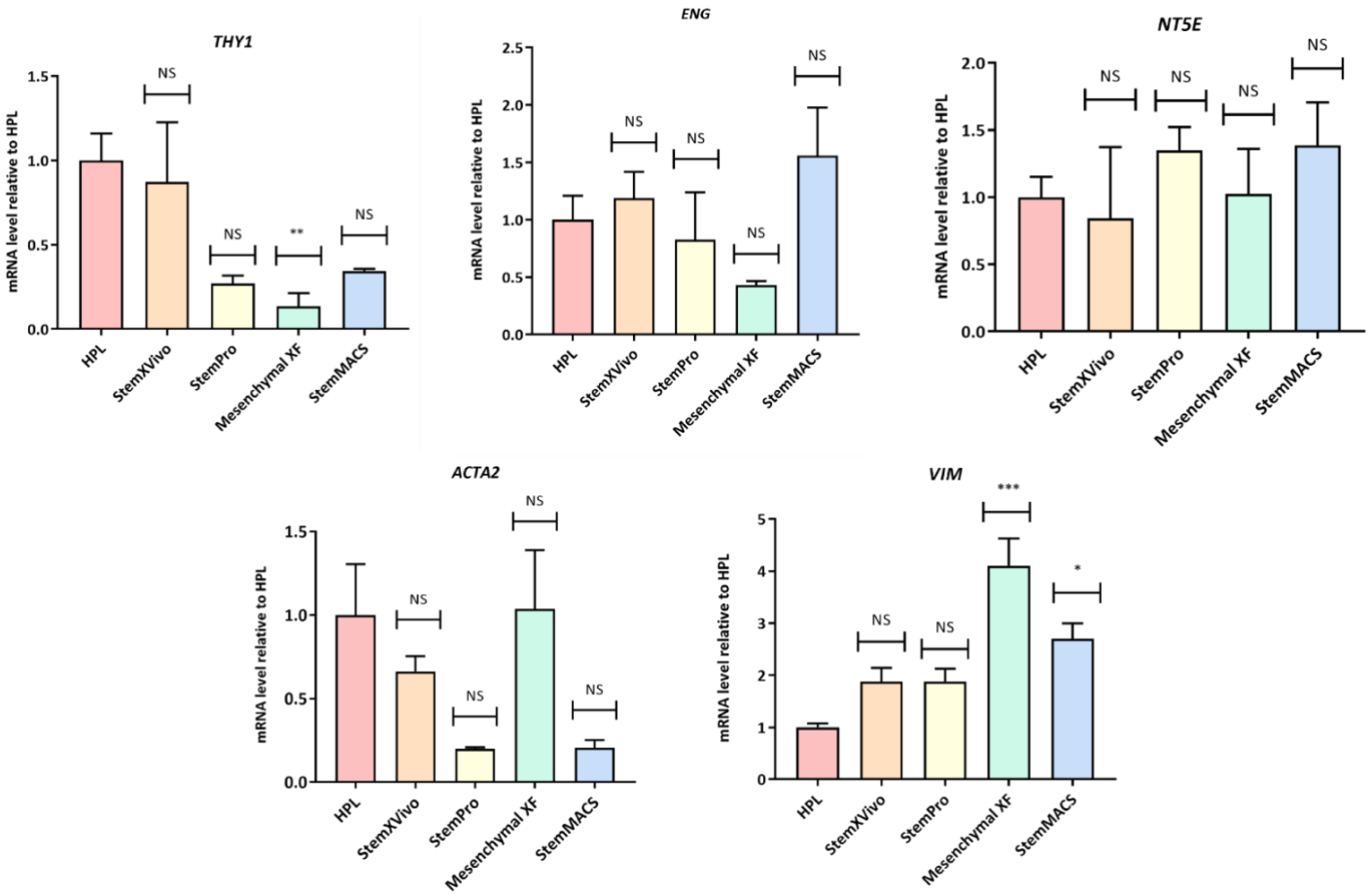

Figure 21. RT-qPCR of CS-MSC expression in xeno-free and chemically defined media HPL, Stem X Vivo, StemPro, Mesenchymal XF and StemMACS with mRNA levels relative to HPL. RT-qPCR was performed for the following genes: *ENG*, *THY1*, *NT5E*, *VIM* and *ACTA2*. Statistically significant values from unpaired t-tests represent (NS = not significant, * $P \leq = 0.05$ ** = $P \leq 0.01$, *** $P \leq 0.001$). Data are shown as mean ± standard deviation. One replicate of RT-qPCR was conducted in order to determine levels of gene expression in five pooled donors.

3.3 Culture of BM-MSCs in HPL media

3.3.1 Morphology of BM-MSCs assessed with phase contrast imaging

Figure 22. BM-MSCs cultured in DMEM/F-12 supplemented with 10% HPL appeared to proliferate at a steady rate between day 1 and 3, approximately reaching 80% confluence at day 7. BM-MSCs appear to look larger and have a spindle-like morphology similar to CS-MSCs cultured in HPL media.

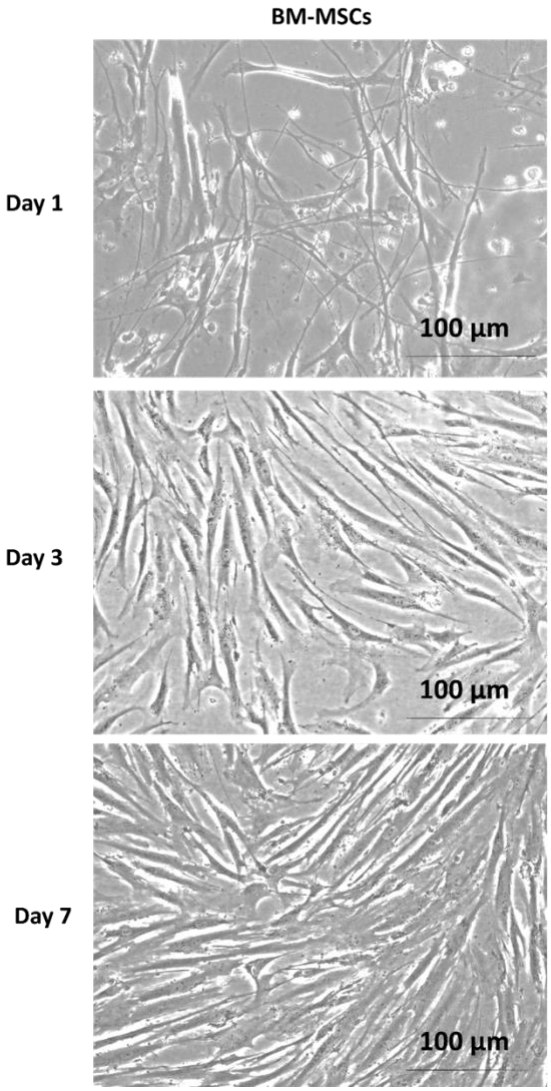

Figure 22. Cell morphology of BM-MSCs cultured in DMEM/F-12 supplemented with 10% HPL at P6. Phase Contrast Images taken on Days 1, 3 and 7 at magnification x10. Scale bar = 100 µm.

3.3.2 Cell viability assessment

Figure 23. The BM-MSCs did not seem to proliferate at high levels in HPL media when compared to CSMSCs cultured in HPL media at day 1. Furthermore, BM-MSCs would have been subject to further cell viability analysis at days 3 and 7, however the assay produced negative results.

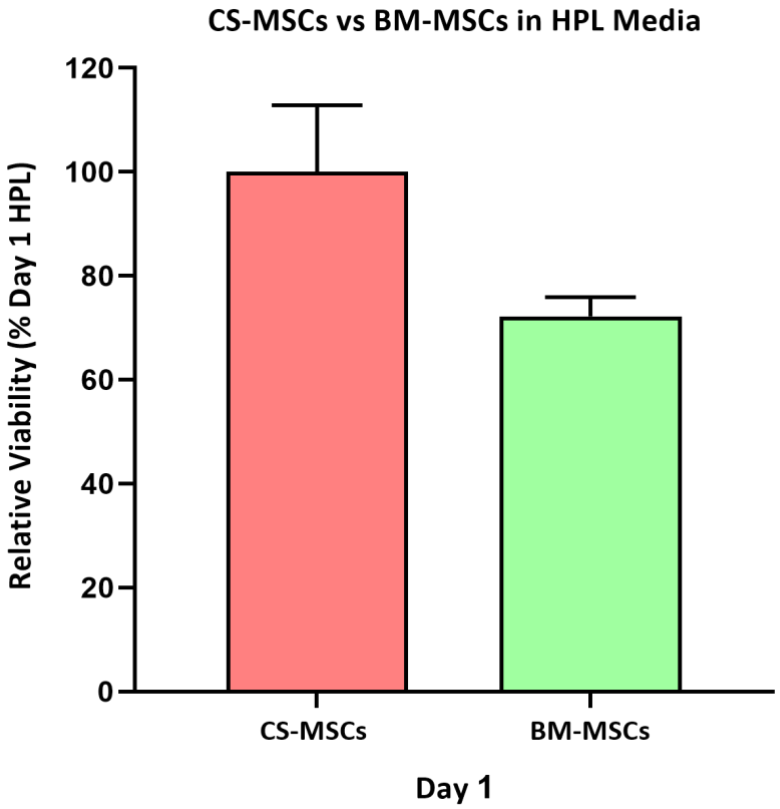

Figure 23. Comparison of CS-MSCs with BM-MSCs cultured in HPL at Day 1. Cells were subject to analysis using Presto Blue Reagent. The percentage of viable cells to Day 1 HPL was calculated. Data are shown as mean ± standard deviation. One replicate of the presto blue assay was conducted in order to determine cell viability across three pooled donors.

3.3.2.1 BM-MSC Marker expression using Immunocytochemistry

Figure 16 and Figure 17. Low levels of the positive marker $CD105^+$ appear to have been expressed by BM-MSCs in HPL media in comparison to CS-MSCs in HPL media. Additionally, low levels of the negative marker $CD34^-$ are expressed by BM-MSCs similarly to CS-MSCs. Levels of $CD73^+$ and $CD90^+$ also remain low in BM-MSCs with significant levels of background staining. Cell morphology cannot be compared to CS-MSCs as the BM-MSCs appear to be unhealthy and not proliferating well. A slightly higher level of the myofibroblast marker α-SMA is present in the BM-MSCs when compared to CS-MSCs. Levels of ALDH3A1 are also lower in BM-MSCs when compared to CS-MSCs. Staining for Vimentin and actin also shows the morphological differences of the BM-MSCs compared to CS-MSCs. CS-MSCs in HPL have the morphology of MSCs due to their spindle like shape, which the BM-MSCs do not possess as they look unhealthy in HPL.

3.3.3 Activation of BM-MSCs and quantification of cytokines released by ELISA

Figure 24. To investigate whether BM-MSCs were releasing soluble factors, or if they were using factors present in media only, the BM-MSC culture media of HPL was collected and compared against CS-MSCs. Constitutive expression of IL-1β, IL-6, IL-8, FGF2, TGF-β1, EGF, PEDF and HGF was detected in both BM-MSCs and CS-MSCs although levels secreted varied between the media. Overall, low levels of the pro-inflammatory cytokine IL- 1β was used up from the HPL media that BM-MSCs and HPL CS-MSCs were cultured in (mean: BM-MSCs = 2.421 pg/mL, CS-MSCs = 0.604 pg/mL). Both BM-MSCs and CS-MSCs additionally produced the cytokine IL-6 at high levels in the HPL media (mean: BM-MSCs = 1058.956 pg/mL, CS-MSCs = 1089.090 pg/mL). Pro-inflammatory IL-8 was secreted by both BM-MSCs and CS-MSCs in HPL media with CS-MSCs producing a significantly higher amount (mean: BM-MSCs = 32.937 pg/mL, CS-MSCs = 1244.784 pg/mL).

FGF2 was present in the HPL media (mean: BM-MSCs = 63.296 pg/mL, CS-MSCs = 26.541 pg/mL) and cells appeared to be using the growth factor (mean: BM-MSCs = 13.609, CS-MSCs = 19.736).

TGF- β1 was present in high levels in the HPL medium (mean: BM-MSCs = 4009.101 pg/mL, HPL = 4425.858 pg/mL) and cells appeared to be using the growth factor (mean: BM-MSCs = 1706.940 pg/mL, CS-MSCs = 2921.969 pg/mL).

EGF appeared to be present in the HPL media (mean: BM-MSCs = 103.628 pg/mL, CS-MSCs = 93.166 pg/mL). CS-MSCs appear to have used a significantly higher amount of EGF in comparison to BM-MSCs (mean: BM-MSCs = 5.275 pg/ML, CS-MSCs = 30.639 pg/mL).

PEDF was present at high levels in the HPL media (mean: BM-MSCs = 7299.72 pg/Ml, CS-MSCs = 5964.928 pg/mL). BM-MSCs appear to have used slightly more of the PEDF in comparison to CS-MSCs (mean: BM-MSCs = 5542.500 pg/mL, CS-MSCs = 5181.188 pg/mL).

HGF appears to be in the HPL media (mean: BM-MSCs = 149.762 pg/mL, CS-MSCs = 178.934 pg/mL) and is additionally produced by BM-MSCs (189.445 pg/mL) and not CS-MSCs.

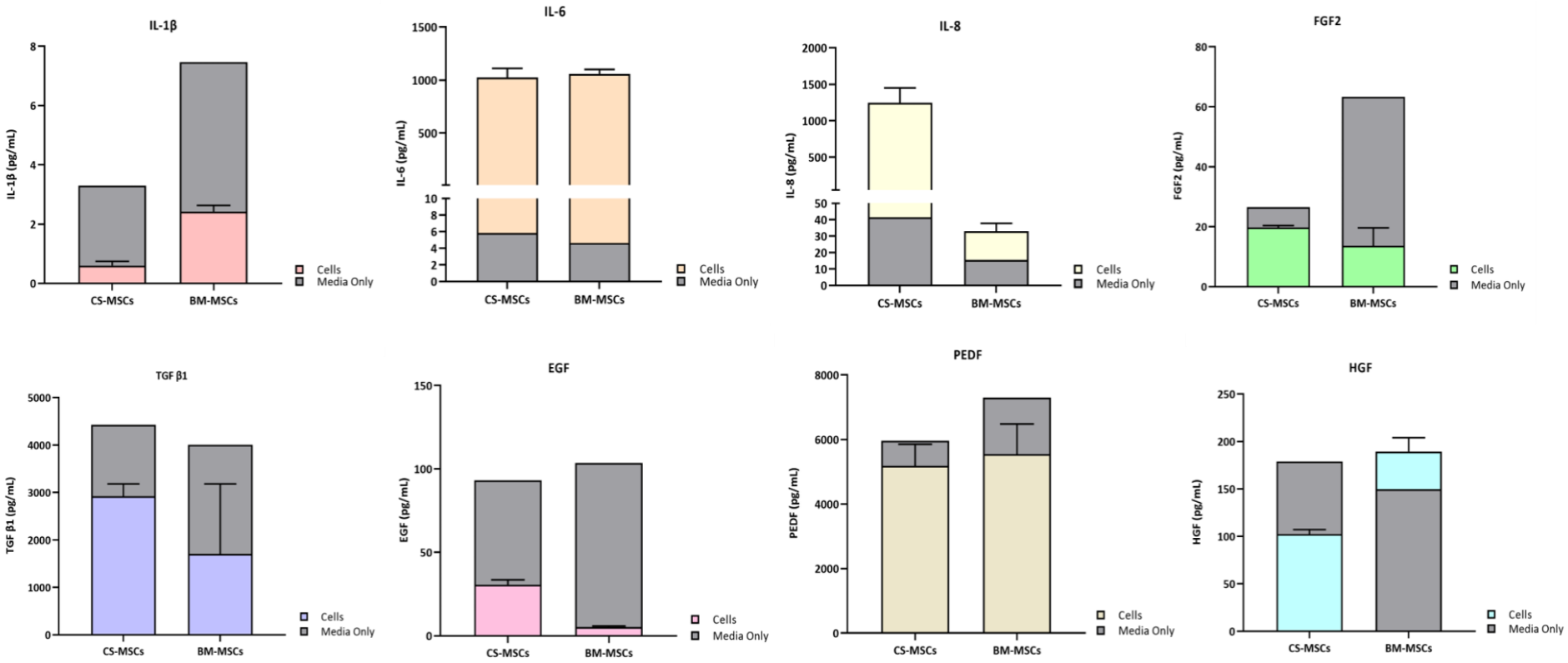

Figure 24. Presence of immunomodulatory cytokines was determined using Enzyme-Linked Immunosorbent Assay (ELISA). Cytokines tested for: IL- β, IL-6, IL-8, TGF- β1, EGF, PEDF, HGF, FGF2. One replicate to determine levels of cytokines and growth factors was conducted using ELISA across three pooled donors.

3.3.4 Potential Media Cytotoxicity

Figure 25. BM-MSCs and CS-MSCs assessed by ToxiLight™ and LDH assays indicated no statistically significant difference in percentage relative toxicity levels to HPL. BM-MSCs however exerted higher levels of toxicity for both assays, indicating that the cells were unhealthy in the HPL media.

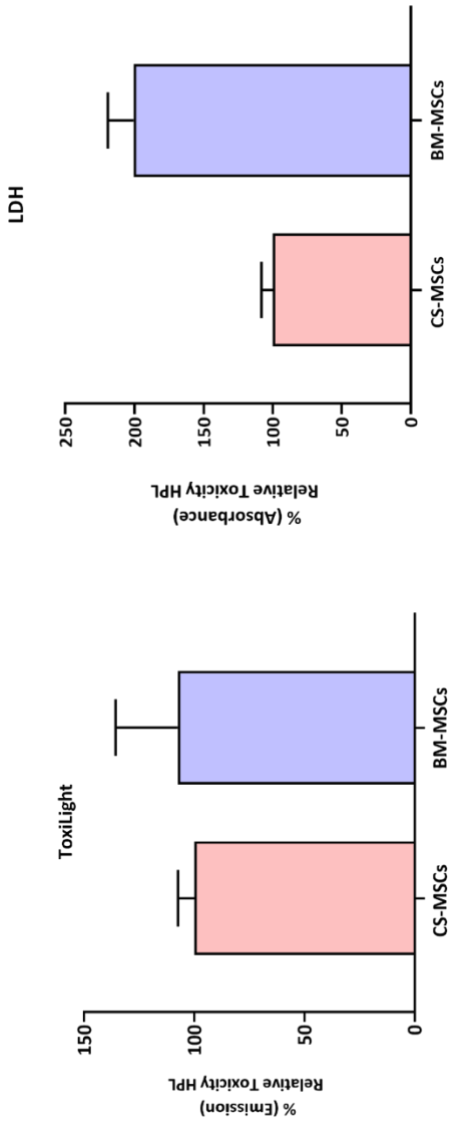

Figure 25. Relative toxicity levels in ToxiLight and LDH assays to the relative toxicity of HPL. Relative percentage emission for BM-MSCs and CS-MSCs. Data are shown as mean ± standard deviation. One replicate of LDH was conducted across three pooled donors to determine relative toxicity.

4 Discussion

4.1 CS-MSCs cultured in Foetal Bovine Serum vs Human Platelet Lysate

In recent years, characterisation of MSCs has become of particular interest due to their therapeutic efficacy. Moreover, CS-MSCs have significant potential in the ophthalmic and regenerative medical field as these cells play a crucial role in corneal regeneration and wound healing [107] . In this project, CS-MSCs cultured in FBS and HPL were characterised for MSC properties and their ability to maintain characteristics with reference to the ISCT MSC marker criteria. Previous research has shown that P4 is considered the optimal passage for the investigation of phenotype, genotype and an increase in would healing potential in comparison to cells at P2 [108].

The project highlights key interest in HPL as a substitute for FBS in culture media for the expansion of CS-MSCs. Media containing HPL has been shown to preserve phenotype of CS-MSCs when compared with FBS. Some differences arise in terms of the cytokines and chemokines secreted, suggesting functional differences between CS-MSCs supplemented with FBS and HPL. This must be investigated prior to clinical translation. The possibility to use animal-free serum culture media has been demonstrated in recent studies by replacing FBS with human-derived supplements such as HPL or human serum [109]. This project clearly demonstrates that the presence of HPL is no different for the expansion of CS-MSCs and can be used to substitute the standard expansion media containing FBS.

To assess MSC phenotype in FBS and HPL through analysis of $CD105^{+}$, $CD90^{+}$ and where $CD34^{-}$ was a negative MSC marker. Both $CD105^{+}$ and $CD90^{-}$ were positively expressed on the population of cells in FBS and HPL [figure 10]. It is important to mention that these markers are also associated with fibroblasts and possess characteristics such as elongated, spindle-shaped morphology as supported by phase contrast images [Figure 6 and Figure 7][110]. Results show that CS-MSCs from donors 1 to 5 in DMEM/F-12 supplemented with 10% FBS proliferate rapidly at day 1, and then plateau at days 3 and 7, whereas CS-MSCs from donors 2 to 5 in DMEM/F-12 supplemented with 10% HPL take longer to proliferate between days 1 and 3, but reach a similar level of confluence at day 7 when compared to FBS. This could be due to HPL containing growth factors such as transforming growth factor (TGF), epidermal growth factor (EGF) and platelet-derived growth factor (PDGF) [111]. These growth factors have previously been demonstrated by Hemeda et al to induce an enhanced rate in the proliferation of MSCs and are able to maintain their multilineage differentiation potential under cell culture in the absence of FBS [81].

Although $CD34^{-}$ is characterised as a haematopoietic stem cell marker, there have been numerous conflicting debates in research. Previous studies have shown that extracted stromal cells from various

tissue sources which did not undergo cell passage and cell culture possessed $CD34^+$ positive cells [112], [113]. In addition to this, other research has shown that keratocytes extracted from the corneal stroma and cultured in serum containing media contained populations of the identifiable MSC markers$CD105^+$, $CD90^+$, $CD73^+$ and $CD34^+$ concluding that $CD34^+$ expression can be determined in MSC populations. As CS-MSCs in this project were analysed at P4, negative $CD34^-$ expression from flow cytometry is supported by literature, indicating negative expression at P3 [112].

CS-MSCs cultured in both FBS and HPL constitutively expressed MSC markers as can be seen in figure 9 and figure 10. Both flow cytometry and immunocytochemistry demonstrated the positive expression of MSC markers $CD105^+$ and $CD90^+$. Flow cytometry histograms from figure 9 give a visual representation of isotype control (red) and marker expression (green) with no apparent difference detected with any marker. Additionally, Percentage relative mean fluorescence from figure 11 is supported by Matthyssen et al as flow cytometry analysis also shows no significant difference in MSC surface markers $CD105^+$ and $CD90^+$, and $CD34^-$ showed less than 1.5% positivity in CS-MSCs cultured in 10% FBS vs 10% HPL.

Immunocytochemistry additionally supports this data as can be seen from figure 10. Expression of $CD105^+$ and $CD90^+$ is maintained, with low detection of $CD34^-$. Immunocytochemistry was also utilised to analyse the expression of ALDH3A1 and the myofibroblast marker α-SMA. High levels of ALDH3A1 were detected in HPL [figure 10D] and moderate levels in FBS [figure 10C] with positive expression on almost every cell. ALDH3A1 is known to be a corneal crystallin responsible for maintaining corneal transparency. Previous *in vivo* studies using rat models subject to chemical alkaline burns demonstrated that a reduced expression of this protein can compromise corneal transparency [114]. α-SMA which is associated with the transformation of keratocytes into myofibroblasts was also positively expressed on some cells in both FBS [figure 10G] and HPL [figure 10H] Less expression seems to be present on CS-MSCs in HPL media due to the higher concentration of HGF [figure 12]. Other research has also shown that MSCs inhibit the expression of opacity inducing α-SMA and its inducer TGF-β1 in the injured cornea by secreting HGF [115].

Vimentin and phalloidin staining were additionally used for structural analysis of CS-MSCs cultured in FBS and HPL including cell morphology and composition of the actin cytoskeleton [figure 10W and figure 10X]. The data shows that at P4, CS-MSCs are evenly spread out with cells cultured in HPL adopting a more spindle-shaped morphology. Phalloidin staining indicates that the actin cytoskeleton remains intact. Other studies have demonstrated that at later passages, phalloidin staining diminishes indicating a breakdown of the actin cytoskeleton. This has been linked with cell aging, where collagen fibrils in aging become fragmented [116]. RT-qPCR analysis also supported immunocytochemistry with

no significant difference observed in gene expression except for *ACTA2* in HPL (** = $P \leq 0.01$). This correlates with α-SMA expression in HPL as levels were lower in comparison with FBS.

A number of growth factors have been identified in platelet concentrations [103],[117]. Among these, TGF-β1, PEDF and FGF2 have been shown to play crucial roles in both differentiation and proliferation of CS-MSCs ELISAs were used to measure concentrations of eight cytokines (IL-1B, IL-6, IL-8, FGF2, TEGF-β1, EGF, PEDF and HGF) in CS-MSC supernatants in comparison with corresponding media. All CS-MSC supernatants contained IL-6 and IL-8 at variable levels. The other cytokines IL-1B, FGF2, TEG-B1, EGF, PEDF and HGF were all present in the corresponding fresh HPL media. The presence of HPL increased IL-6 and IL-8 concentrations in comparison to FBS where the only additional cytokine produced was FGF2. Similar results were found by Azouna et al who demonstrated that HPL supplemented media also had increased levels of IL-6 and IL-8 with no detection of FGF2. Secretion of both the pro-inflammatory and hematopoietic cytokine IL-6 and the chemokine IL-8 was increased in CS-MSCs previously expanded in HPL supplemented media as described previously for IL-6 [118]. This indicates that HPL contains strong inductors of such cytokines that could minimise the potential anti-inflammatory activity of CS-MSCs.

Overall, the results from this section have shown no significant difference in phenotypic characterisation of CS-MSCs when cultured in FBS vs HPL. Furthermore, no significant difference was detected in cell viability [figure 8]. As a result, it can be concluded that future work into the development of a cellular therapy using CS-MSCs for corneal diseases should use HPL supplemented media for a step closer towards clinical translation.

4.2 CS-MSCs cultured in Xeno-free and chemically defined media

Vast efforts have been made by researchers and manufacturers to identify an appropriate media composition for MSC culture which are not dependent on FBS supplementation. Among these serum and animal component free serum substitutes, HPL has been studied extensively and was found to increase human MSC proliferation compared to FBS [119]. Many researchers have also reported that MSCs did not display changes in their immunophenotype when cultured in HPL media.

In order for corneal mesenchymal stem cell therapies to be used in clinic, the production of the cellular therapies must comply with cGMP. As major concerns have been raised from the use of ill-defined FBS from an ethical and animal welfare point of view, this has led to GMP regulators demanding Xeno-free culture protocols [120]. In this project, HPL was also used as a control media to culture CS-MSCs in three Xeno-free media: Stem X Vivo, Mesenchymal XF, StemMACS XF and one chemically defined media: StemPro MSC SFM XF. All xeno-free and chemically defined media stated that separate solutions were not required to facilitate cell attachment. Unfortunately, CS-MSCs did not adhere well to tissue culture plastic and therefore a 0.1% gelatin solution was used to coat all flasks.

The majority of serum-free formulations claim equivalent cell populations compared with serum contain media. This does not correlate with results obtained in this project. Despite phase contrast images from figure 14 showing the cell population with spindle-like morphological characteristics of CS-MSCs at day 1 and day 3, flow cytometry and immunocytochemistry did not support this. Figure 16 illustrates that the MSC markers for $CD73^{+}$, $CD90^{+}$, $CD105^{+}$, with negative expression of $CD34^{-}$ were relatively low in StemPro, Mesenchymal XF and StemMACS. The serum containing control media HPL and high-quality factors of Stem X Vivo induced similar levels of expression at higher levels. Immunocytochemistry [figure 17] revealed no difference in the expression of MSC markers $CD73^{+}$, $CD90^{+}$, $CD105^{+}$, with negative expression of $CD34^{-}$. Cells cultured in Stem X Vivo, Stem Pro MSC, Mesenchymal XF and StemMACS did not exhibit spindle-like morphology and were different in size and shape. Immunocytochemistry was again utilised to analyse the expression of ALDH3A1 and the myofibroblast marker α-SMA. Figure 18.1 indicates that α-SMA was only expressed by a few cells, with ALDH3A1 expressed by almost all cells [figure 18]. Phalloidin staining of the actin cytoskeleton also remained well intact and cells evenly spaced out possessing spindle morphology. Stem X Vivo, Stem Pro MSC SFM and StemMACS XF contained slightly higher levels of α-SMA expression, with similar levels of ALDH3A1 and structural staining for Vimentin and Phalloidin. Staining was not consistent in Mesenchymal XF as levels of MSC marker expression were very low. In addition to this, structural staining revealed low levels of Vimentin [figure 18.22] and actin [figure 18.28], suggesting degradation of the actin cytoskeleton and absence of spindle morphology.

Previous studies have compared different SFM media formulations for MSC culture and have shown that the media of choice can increase cell proliferation and differentiation [121]. In this project, Presto Blue cell viability at day 1 HPL [Figure 8] revealed no difference between the media, with the exception of Stem X Vivo which seemed to proliferate cells at a higher level due to its composition of high quality factors.

Additionally, figure 20 indicates levels of IL-1β were secreted across all xeno-free media (with the exception of StemMACS XF) as demonstrated by Jeong et al. IL-1β is required in normal wound repair due to its role in the migration of immune cells to the corneal wound via the production of proteolytic enzymes [122]. Additionally, there were high levels of pro-inflammatory IL-6 and IL-8 secretion. FGF2 was only produced in the Mesenchymal XF media. In comparison to other research where long term cell culture of MSCs induced an increase in the regeneration of tissues [123]. It has also been reported that TGF-β1 is an important factor in promoting corneal wound healing, and serves as a secretory immune modulator of MSCs [124]. EGF was also secreted by HPL, Stem X Vivo and Mesenchymal Expansion Media which plays an important role in regulating cell proliferation and differentiation during corneal epithelium wound healing. It has been reported that EGF synergizes with TGF-β1 in rabbit corneal keratocytes on the migration of myofibroblasts [125]. HGF is produced by MSCs and operates as a key molecule for tissue regeneration and renewal. During corneal injury, HGF is primarily secreted by stromal fibroblasts and promotes epithelial wound healing [126]. This correlates with HGF data in this project as all CS-MSCs across the five media secreted the growth factor. Other research has also indicated that CS-MSC derived PEDF is responsible for anti-inflammatory effects by inhibiting macrophage recruitment and activation. Previous researchers have demonstrates that CS-MSC derived PEDF is not only involved in the activation of macrophage apoptosis, but also contributes to the development of anti-inflammatory macrophages which function by removing immune cells and granulated tissue [114].

As can be seen in figure 21, there was no statistically significant difference determined for the genes *ENG*, *NT5E* and *ACTA2*. *THY1* ($CD90^+$) was significantly different for Mesenchymal XF (** = $P \leq 0.01$ and *VIM* was significantly different for Mesenchymal XF (*** = $P \leq 0.001$) and StemMACS XF (* = $P \leq 0.05$). These results correlated with immunocytochemistry with low levels of marker expression detected. Additionally, figure 19 shows that cytotoxicity levels in all media compared to HPL for ToxiLight and LDH were statistically significant ($P \leq 0.0001$) with Stem X Vivo containing the lowest levels of toxicity.

The results obtained from this section concluded that Stem X Vivo was the best media for the culture of CS-MSCs. CS-MSCs were able to maintain morphology and phenotype in addition to the media containing the lowest level of potential toxicity. Despite no statistical significance between the genes

THY1, ENG, *NT5E*, *ACTA2* and *VIM* CS-MSCs in Stem X Vivo secreted specific cytokines at higher concentrations for IL-1β, TGF-β1, EGF, PEDF and HGF in comparison to HPL. As Stem X Vivo and HPL maintain CS-MSC characteristics at similar levels, HPL should be investigated further for potential clinical translation and projected large-scale production.

4.3 BM-MSCs cultured in HPL media

There has been significant interest in the culture of BM-MSCs in HPL media. Previous research has suggested that BM-MSCs expanded in 10% supplemented HPL media were multipotent as they were able to differentiate into four mesenchymal pathways (adipogenic, osteogenic, chrondogenic and vascular smooth muscle function) [127]. BM-MSCs have been shown to retain these pathways in HPL media and shorten expansion culture duration in comparison to CS-MSCs.

This project aimed to demonstrate that BM-MSCs were able to proliferate at a higher level than CS-MSCs in HPL media. Unfortunately, not all results obtained correlate with this research. BM-MSCs required adhesion to flasks using gelatin coating but grew at extremely slow rates. It took approximately three weeks between passages and high confluence levels were not obtained. Figure 22 demonstrates how BM-MSCs acquire a spindle morphology similar to CS-MSCs in HPL which became more dendritic in appearance by day 7. In contrast to these images, cell viability analysis revealed that BM-MSCs were not proliferating in the HPL media when compared with CS-MSCs in HPL. Figure 23 shows at day 1 of analysis, BM-MSCs are at approximately 70% viability, indicating the cells were not surviving well. Similarly, ELISA concentrations from figure 24 show an increase secretion of pro-inflammatory IL-1β and IL-6 with a reduction in IL-8 in BM-MSCs. Another key difference is that BM-MSCs additionally secreted HGF when CS-MSCs in HPL did not. This is due to HGF playing a crucial role in haematopoiesis [128]. Potential media toxicity levels from ToxiLight and LDH [figure 25] also indicated that BM-MSCs in HPL media were not able to grow or proliferate.

As previously mentioned, other research has demonstrated the benefits of culturing BM-MSCs in HPL media with rapid levels of cell proliferation. Unfortunately, the results from this set of experiments suggest that HPL media for the culture of BM-MSCs is unsuitable. Further investigation into culturing BM-MSCs in tissue culture plastic without the use of bovine gelatin should be conducted. Fibronectin has previously been shown to enhance the proliferation of BM-MSCs in HPL media and thus enabled phenotypic comparison with CS-MSCs cultured in HPL media [127].

5 Future Work

As samples were obtained from two different locations (Manchester Eye Bank and Nottingham University Hospitals), this adds an element of variability of the donor source. Tissue viability may have been affected due to different lengths of transport and storage before use resulting in decreased cell potency. In addition to this, there was significant variability in the process of isolating enough cells from each donor sample for the project. On numerous occasions extracted cells at P0 would not become confluent enough to passage, thus causing a delay in experimental procedures. It was therefore decided to pool donors together in order to accumulate the desired number of cells in order to continue with the project and split the cells across $n = 5$ to fulfil any statistical analysis for the xeno-free experiments. It was also unknown whether the donor samples had any pre-existing medical conditions which may have contributed towards lack of cell growth/possible infection. Future experiments should take into consideration a larger number of donors including donors with specific age ranges to further minimize donor variability.

The project has positively impacted the field due to lack of research into the comparison of FBS and HPL alternatives in order to take a step closer to clinical translation. More investigation is essential in order to identify which xeno-free media is most effective and whether it would be feasible to produce the GMP product.

Further investigation into this project would be significantly beneficial to develop an optimal xeno-free cell culture media. One of the main difficulties encountered during the project was ensuring CS-MSCs and BM-MSCs adhered to the tissue culture plastic in the xeno-free and chemically defined media. The same problem was also encountered when culturing BM-MSCs in HPL media. This was resolved by coating plates with bovine gelatin, however this is not a xeno-free product and thus a severe limitation. If conducting a longitudinal study, the best method would be to test each media and see if cells are able to adhere onto tissue culture plastic without the addition of gelatin however this can be costly in terms of reagents.

It would therefore be advantageous to use a xeno-free derived gelatin to coat flasks prior to cell culture as well as a GMP grade collagenase for CS-MSC isolation. In addition to this, future experiments should be conducted on culturing CS-MSCs and BM-MSCs in Stem X Vivo; the media which was highlighted in the project as the best xeno-free alternative. A comparison between characterisation of CS-MSCs and BM-MSCs cultured on xeno-free gelatin in Stem X Vivo could then be subject to analysis at P6 (a higher number of corneal rim donors should also be used to reduce donor variability)

with the same experimental procedures used throughout this project for a step towards true clinical translation.

6 References

[1] Meek KM, Knupp C. Corneal structure and transparency. Prog Retin Eye Res 2015;49:1–16. doi:10.1016/j.preteyeres.2015.07.001.

[2] Nagymihaly R, Vereb Z, Albert R, Sidney L, Dua H, Hopkinson A, et al. Cultivation and characterisation of the surface markers and carbohydrate profile of human corneal endothelial cells. Clin Experiment Ophthalmol 2017;45:509–19. doi:10.1111/ceo.12903.

[3] Galletti JG, Guzman M, Giordano MN. Mucosal immune tolerance at the ocular surface in health and disease. Immunology 2017;150:397–407. doi:10.1111/imm.12716.

[4] Lucas T, Waisman A, Ranjan R, Roes J, Krieg T, Muller W, et al. Differential roles of macrophages in diverse phases of skin repair. J Immunol 2010;184:3964–77. doi:10.4049/jimmunol.0903356.

[5] Dua HS, Faraj LA, Said DG, Gray T, Lowe J. Human corneal anatomy redefined: a novel pre-Descemet's layer (Dua's layer). Ophthalmology 2013;120:1778–85. doi:10.1016/j.ophtha.2013.01.018.

[6] Wu J, Du Y, Watkins SC, Funderburgh JL, Wagner WR. The engineering of organized human corneal tissue through the spatial guidance of corneal stromal stem cells. Biomaterials 2012;33:1343–52. doi:10.1016/j.biomaterials.2011.10.055.

[7] Francis AW, Kagemann L, Wollstein G, Ishikawa H, Folz S, Overby DR, et al. Morphometric analysis of aqueous humor outflow structures with spectral-domain optical coherence tomography. Invest Ophthalmol Vis Sci 2012;53:5198–207. doi:10.1167/iovs.11-9229.

[8] Bonanno JA. Molecular mechanisms underlying the corneal endothelial pump. Exp Eye Res 2012;95:2–7. doi:10.1016/j.exer.2011.06.004.

[9] Flanagan JL, Willcox MDP. Role of lactoferrin in the tear film. Biochimie 2009;91:35–43. doi:10.1016/j.biochi.2008.07.007.

[10] Freeman RD. Oxygen consumption by the component layers of the cornea. J Physiol 1972;225:15–32.

[11] Taylor AW. Ocular Immune Privilege and Transplantation. Front Immunol 2016;7:37. doi:10.3389/fimmu.2016.00037.

[12] Ingulli E. Mechanism of cellular rejection in transplantation. Pediatr Nephrol 2010;25:61–74. doi:10.1007/s00467-008-1020-x.

[13] Hori J. Mechanisms of immune privilege in the anterior segment of the eye: what we learn from corneal transplantation. J Ocul Biol Dis Infor 2008;1:94–100. doi:10.1007/s12177-008-9010-6.

[14] Paunicka K, Chen PW, Niederkorn JY. Role of IFN-γ in the establishment of anterior chamber-associated immune deviation (ACAID)-induced CD8+ T regulatory cells. J Leukoc Biol 2012;91:475–83. doi:10.1189/jlb.0311173.

[15] Shaheen BS, Bakir M, Jain S. Corneal nerves in health and disease. Surv Ophthalmol 2014;59:263–85. doi:10.1016/j.survophthal.2013.09.002.

[16] Rosenthal P, Borsook D, Moulton EA. Oculofacial Pain: Corneal Nerve Damage Leading to Pain Beyond the Eye. Invest Ophthalmol Vis Sci 2016;57:5285–7. doi:10.1167/iovs.16-20557.

[17] Vega-Estrada A, Alio JL. The use of intracorneal ring segments in keratoconus. Eye Vis (London, England) 2016;3:8. doi:10.1186/s40662-016-0040-z.

[18] Kulkarni BB, Tighe PJ, Mohammed I, Yeung AM, Powe DG, Hopkinson A, et al. Comparative transcriptional profiling of the limbal epithelial crypt demonstrates its putative stem cell niche characteristics. BMC Genomics 2010;11:526. doi:10.1186/1471-2164-11-526.

[19] Holthofer B, Windoffer R, Troyanovsky S, Leube RE. Structure and function of desmosomes. Int Rev Cytol 2007;264:65–163. doi:10.1016/S0074-7696(07)64003-0.

[20] Torricelli AAM, Singh V, Santhiago MR, Wilson SE. The corneal epithelial basement membrane: structure, function, and disease. Invest Ophthalmol Vis Sci 2013;54:6390–400. doi:10.1167/iovs.13-12547.

[21] Prina E, Mistry P, Sidney LE, Yang J, Wildman RD, Bertolin M, et al. 3D Microfabricated Scaffolds and Microfluidic Devices for Ocular Surface Replacement: a Review. Stem Cell Rev 2017;13:430–41. doi:10.1007/s12015-017-9740-6.

[22] Kenyon KR. Morphology and pathologic responses of the cornea to disease. Cornea Sci Found Clin Pract G Smolin RA Thoft, Ed Little, Brown Co, Bost 1987:63–98.

[23] Wilson SE, Hong J-W. Bowman's layer structure and function: critical or dispensable to corneal function? A hypothesis. Cornea 2000;19:417–20.

[24] Sridhar MS. Anatomy of cornea and ocular surface. Indian J Ophthalmol 2018;66:190–4. doi:10.4103/ijo.IJO_646_17.

[25] Beales MP, Funderburgh JL, Jester J V, Hassell JR. Proteoglycan synthesis by bovine keratocytes and corneal fibroblasts: maintenance of the keratocyte phenotype in culture. Invest Ophthalmol Vis Sci 1999;40:1658–63.

[26] Van Buskirk EM. The anatomy of the limbus. Eye (Lond) 1989;3 (Pt 2):101–8. doi:10.1038/eye.1989.16.

[27] Hashmani K, Branch MJ, Sidney LE, Dhillon PS, Verma M, McIntosh OD, et al. Characterization of corneal stromal stem cells with the potential for epithelial transdifferentiation. Stem Cell Res Ther 2013;4:75.

[28] WHO. WHO | 12 October 2017: World Sight Day. WHO 2018.

[29] NHS. General Ophthalmic Services activity statistics - England, year ending 31 March 2015 - NHS Digital n.d. https://digital.nhs.uk/data-and-information/publications/statistical/general-ophthalmic-services-activity-statistics/general-ophthalmic-services-activity-statistics-england-year-ending-31-march-2015 (accessed January 22, 2019).

[30] World Health Org. World Sight Day. 2017 n.d. https://www.who.int/blindness/world_sight_day/2017/en/.

[31] Whitcher JP, Srinivasan M, Upadhyay MP. Corneal blindness: a global perspective. Bull World Health Organ 2001;79:214–21.

[32] Dua HS, Azuara-Blanco A. Autologous limbal transplantation in patients with unilateral corneal stem cell deficiency. Br J Ophthalmol 2000;84:273 LP – 278. doi:10.1136/bjo.84.3.273.

[33] Shimazaki J, Aiba M, Goto E, Kato N, Shimmura S, Tsubota K. Transplantation of human limbal epithelium cultivated on amniotic membrane for the treatment of severe ocular surface disorders. Ophthalmology 2002;109:1285–90.

[34] Kenyon KR, Tseng SC. Limbal autograft transplantation for ocular surface disorders. Ophthalmology 1989;96:703–9.

[35] Miri A, Said DG, Dua HS. Donor site complications in autolimbal and living-related allolimbal transplantation. Ophthalmology 2011;118:1265–71. doi:10.1016/j.ophtha.2010.11.030.

[36] Reinhard T, Spelsberg H, Henke L, Kontopoulos T, Enczmann J, Wernet P, et al. Long-term results of allogeneic penetrating limbo-keratoplasty in total limbal stem cell deficiency. Ophthalmology 2004;111:775–82. doi:10.1016/j.ophtha.2003.07.013.

[37] Solomon A, Ellies P, Anderson DF, Touhami A, Grueterich M, Espana EM, et al. Long-term outcome of keratolimbal allograft with or without penetrating keratoplasty for total limbal stem cell deficiency. Ophthalmology 2002;109:1159–66.

[38] Henderson TR, McCall SH, Taylor GR, Noble BA. Do transplanted corneal limbal stem cells survive in vivo long-term? Possible techniques to detect donor cell survival by polymerase chain reaction with the amelogenin gene and Y-specific probes. Eye (Lond) 1997;11 (Pt 6):779–85. doi:10.1038/eye.1997.204.

[39] Weiner LP. Definitions and Criteria for Stem Cells BT - Neural Stem Cells: Methods and Protocols. In: Weiner LP, editor., Totowa, NJ: Humana Press; 2008, p. 3–8. doi:10.1007/978-1-59745-133-8_1.

[40] Biehl JK, Russell B. Introduction to stem cell therapy. J Cardiovasc Nurs 2009;24:98–105. doi:10.1097/JCN.0b013e318197a6a5.

[41] Ohtaki H, Ylostalo JH, Foraker JE, Robinson AP, Reger RL, Shioda S, et al. Stem/progenitor cells from bone marrow decrease neuronal death in global ischemia by modulation of inflammatory/immune responses. Proc Natl Acad Sci 2008;105:14638 LP – 14643. doi:10.1073/pnas.0803670105.

[42] Orlic D, Kajstura J, Chimenti S, Jakoniuk I, Anderson SM, Li B, et al. Bone marrow cells regenerate infarcted myocardium. Nature 2001;410:701–5. doi:10.1038/35070587.

[43] Mason C, Manzotti E. Regenerative medicine cell therapies: numbers of units manufactured and patients treated between 1988 and 2010. Regen Med 2010;5:307–13.

[44] Mason C, Brindley DA, Culme-Seymour EJ, Davie NL. Cell therapy industry: billion dollar global business with unlimited potential. Regen Med 2011;6:265–72.

[45] Brindley DA, Davie NL, Sahlman WA, Bonfiglio GA, Culme-Seymour EJ, Reeve BC, et al. Promising growth and investment in the cell therapy industry during the first quarter of 2012. Cell Stem Cell 2012;10:492–6.

[46] Zhu Z, Huangfu D. Human pluripotent stem cells: an emerging model in developmental biology. Development 2013;140:705 LP – 717. doi:10.1242/dev.086165.

[47] Pastor WA, Chen D, Liu W, Kim R, Sahakyan A, Lukianchikov A, et al. Naive human pluripotent cells feature a methylation landscape devoid of blastocyst or germline memory. Cell Stem Cell 2016;18:323–9.

[48] Gerecht-Nir S, Itskovitz-Eldor J. The promise of human embryonic stem cells. Best Pract Res Clin Obstet Gynaecol 2004;18:843–52. doi:10.1016/j.bpobgyn.2004.07.004.

[49] UCLA. Induced Pluripotent Stem Cells (iPS) | UCLA Broad Stem Cell Center n.d. https://stemcell.ucla.edu/induced-pluripotent-stem-cells (accessed January 22, 2019).

[50] Takahashi K, Yamanaka S. Induction of pluripotent stem cells from mouse embryonic and

adult fibroblast cultures by defined factors. Cell 2006;126:663–76.

[51] Hussein SMI, Nagy AA. Progress made in the reprogramming field: new factors, new strategies and a new outlook. Curr Opin Genet Dev 2012;22:435–43.

[52] Sobhani A, Khanlarkhani N, Baazm M, Mohammadzadeh F, Najafi A, Mehdinejadiani S, et al. Multipotent Stem Cell and Current Application. Acta Med Iran 2017;55:6–23.

[53] Rong Z, Wang M, Hu Z, Stradner M, Zhu S, Kong H, et al. An effective approach to prevent immune rejection of human ESC-derived allografts. Cell Stem Cell 2014;14:121–30.

[54] Mirzaei H, Sahebkar A, Sichani LS, Moridikia A, Nazari S, Sadri Nahand J, et al. Therapeutic application of multipotent stem cells. J Cell Physiol 2018;233:2815–23. doi:10.1002/jcp.25990.

[55] Haniffa MA, Collin MP, Buckley CD, Dazzi F. Mesenchymal stem cells: the fibroblasts' new clothes? Haematologica 2009;94:258–63. doi:10.3324/haematol.13699.

[56] Friedenstein AJ. Precursor cells of mechanocytes. Int Rev Cytol 1976;47:327–59.

[57] Bartholomew A, Sturgeon C, Siatskas M, Ferrer K, McIntosh K, Patil S, et al. Mesenchymal stem cells suppress lymphocyte proliferation in vitro and prolong skin graft survival in vivo. Exp Hematol 2002;30:42–8.

[58] Di Nicola M, Carlo-Stella C, Magni M, Milanesi M, Longoni PD, Matteucci P, et al. Human bone marrow stromal cells suppress T-lymphocyte proliferation induced by cellular or nonspecific mitogenic stimuli. Blood 2002;99:3838–43.

[59] Glennie S, Soeiro I, Dyson PJ, Lam EW-F, Dazzi F. Bone marrow mesenchymal stem cells induce division arrest anergy of activated T cells. Blood 2005;105:2821–7.

[60] Spaggiari GM, Capobianco A, Abdelrazik H, Becchetti F, Mingari MC, Moretta L. Mesenchymal stem cells inhibit natural killer–cell proliferation, cytotoxicity, and cytokine production: role of indoleamine 2, 3-dioxygenase and prostaglandin E2. Blood 2008;111:1327–33.

[61] Majumdar MK, Thiede MA, Haynesworth SE, Bruder SP, Gerson SL. Human marrow-derived mesenchymal stem cells (MSCs) express hematopoietic cytokines and support long-term hematopoiesis when differentiated toward stromal and osteogenic lineages. J Hematother Stem Cell Res 2000;9:841–8. doi:10.1089/152581600750062264.

[62] Xi J, Yan X, Zhou J, Yue W, Pei X. Mesenchymal stem cells in tissue repairing and regeneration: Progress and future. Burn Trauma 2015;1:13–20. doi:10.4103/2321-3868.113330.

[63] West-Mays JA, Dwivedi DJ. The keratocyte: corneal stromal cell with variable repair phenotypes. Int J Biochem Cell Biol 2006;38:1625–31. doi:10.1016/j.biocel.2006.03.010.

[64] Han K, Lee JE, Kwon SJ, Park SY, Shim SH, Kim H, et al. Human amnion-derived mesenchymal stem cells are a potential source for uterine stem cell therapy. Cell Prolif 2008;41:709–25. doi:10.1111/j.1365-2184.2008.00553.x.

[65] Friedenstein AJ, Chailakhyan RK, Latsinik N V, Panasyuk AF, Keiliss-Borok I V. Stromal cells responsible for transferring the microenvironment of the hemopoietic tissues. Cloning in vitro and retransplantation in vivo. Transplantation 1974;17:331–40.

[66] Branch MJ, Hashmani K, Dhillon P, Jones DRE, Dua HS, Hopkinson A. Mesenchymal stem cells in the human corneal limbal stroma. Invest Ophthalmol Vis Sci 2012;53:5109–16.

[67] Păunescu V, Deak E, Herman D, Siska IR, T˘ anasie G, Bunu C, et al. In vitro differentiation of

human mesenchymal stem cells to epithelial lineage. J Cell Mol Med 2007;11:502–8.

[68] Sidney LE, Branch MJ, Dua HS, Hopkinson A. Effect of culture medium on propagation and phenotype of corneal stroma–derived stem cells. Cytotherapy 2015;17:1706–22.

[69] E.Medicines Agency. Good manufacturing practice | European Medicines Agency n.d. https://www.ema.europa.eu/en/human-regulatory/research-development/compliance/good-manufacturing-practice (accessed January 22, 2019).

[70] Kirouac DC, Zandstra PW. The systematic production of cells for cell therapies. Cell Stem Cell 2008;3:369–81.

[71] B Directive 2001/83/EC of The European Parliament and Council of 6 November 2001 on the Community code relating to medicinal products for human use. n.d.

[72] Sheu J, Klassen H, Bauer G. Cellular manufacturing for clinical applications. Cell-Based Ther. Retin. Degener. Dis., vol. 53, Karger Publishers; 2014, p. 178–88.

[73] I of the Euopean Parliament and of The Council of 16 April 2014 on clinical trials on medicinal products for human use, and repealing Directive 2001/20/EC (Text with EEA relevance). n.d.

[74] Katrin Lutz JB, Brun J, Lutz K, Rolauffs B, Aicher WK. Do we Need Standardized, GMP-Compliant Cell Culture Procedures for Pre-Clinical In vitro Studies Involving Mesenchymal Stem/Stromal Cells? J Tissue Sci Eng 2014;05:1–4. doi:10.4172/2157-7552.1000135.

[75] Giancola R, Bonfini T, Iacone A. Cell therapy: cGMP facilities and manufacturing. Muscles Ligaments Tendons J 2012;2:243.

[76] Whyte W. Cleanroom technology: fundamentals of design, testing and operation. John Wiley & Sons; 2010.

[77] Nagle Jr SC, Anderson RE, Gary ND. Chemically defined medium for the growth of Pasteurella tularensis. J Bacteriol 1960;79:566.

[78] Havenner JA, McCardell BA, Weiner RM. Development of defined, minimal, and complete media for the growth of Hyphomicrobium neptunium. Appl Environ Microbiol 1979;38:18–23.

[79] Hodgson J. To treat or not to treat: that is the question for serum. Nat Biotechnol 1995;13:333.

[80] Jochems CEA, Van Der Valk JBF, Stafleu FR, Baumans V. The use of fetal bovine serum: ethical or scientific problem? ATLA-NOTTINGHAM- 2002;30:219–28.

[81] Hemeda H, Giebel B, Wagner W. Evaluation of human platelet lysate versus fetal bovine serum for culture of mesenchymal stromal cells. Cytotherapy 2014;16:170–80.

[82] Tekkatte C, Gunasingh GP, Cherian KM, Sankaranarayanan K. “Humanized” stem cell culture techniques: the animal serum controversy. Stem Cells Int 2011;2011.

[83] Medicines Agency E. Guideline on the responsibilities of the sponsor with 5 regard to handling and shipping of investigational 6 medicinal products for human use in accordance with 7 Good Clinical Practice and Good Manufacturing Practice. 2018.

[84] Jayme DW, Epstein DA, Conrad DR. Fetal bovine serum alternatives. Nature 1988;334:547–8.

[85] Sundin M, Ringdén O, Sundberg B, Nava S, Götherström C, Le Blanc K. No alloantibodies against mesenchymal stromal cells, but presence of anti-fetal calf serum antibodies, after transplantation in allogeneic hematopoietic stem cell recipients. Haematologica 2007;92:1208–15.

[86] Horwitz EM, Gordon PL, Koo WKK, Marx JC, Neel MD, McNall RY, et al. Isolated allogeneic bone marrow-derived mesenchymal cells engraft and stimulate growth in children with osteogenesis imperfecta: Implications for cell therapy of bone. Proc Natl Acad Sci 2002;99:8932–7.

[87] Gospodarowicz D, Ferrara N, Schweigerer L, Neufeld G. Structural characterization and biological functions of fibroblast growth factor. Endocr Rev 1987;8:95–114.

[88] Heldin C-H, Betsholtz C, Johnsson A, Nistér M, Ek B, Rönnstrand L, et al. Platelet-derived growth factor: mechanism of action and relation to oncogenes. J Cell Sci 1985;1985:65–76.

[89] Carpenter G, Cohen S. Epidermal growth factor. Annu Rev Biochem 1979;48:193–216.

[90] van der Valk J, Mellor D, Brands R, Fischer R, Gruber F, Gstraunthaler G, et al. The humane collection of fetal bovine serum and possibilities for serum-free cell and tissue culture. Toxicol In Vitro 2004;18:1–12.

[91] Even MS, Sandusky CB, Barnard ND. Serum-free hybridoma culture: ethical, scientific and safety considerations. TRENDS Biotechnol 2006;24:105–8.

[92] Erickson GA, Bolin SR, Landgraf JG. Viral contamination of fetal bovine serum used for tissue culture: risks and concerns. Dev Biol Stand 1991;75:173–5.

[93] Fekete N, Gadelorge M, Fürst D, Maurer C, Dausend J, Fleury-Cappellesso S, et al. Platelet lysate from whole blood-derived pooled platelet concentrates and apheresis-derived platelet concentrates for the isolation and expansion of human bone marrow mesenchymal stromal cells: production process, content and identification of active comp. Cytotherapy 2012;14:540–54.

[94] Rauch C, Feifel E, Amann E-M, Spotl HP, Schennach H, Pfaller W, et al. Alternatives to the use of fetal bovine serum: human platelet lysates as a serum substitute in cell culture media. ALTEX 2011;28:305–16.

[95] Mellor DJ, Gregory NG. Responsiveness, behavioural arousal and awareness in fetal and newborn lambs: experimental, practical and therapeutic implications. N Z Vet J 2003;51:2–13.

[96] Von Bonin M, Stölzel F, Goedecke A, Richter K, Wuschek N, Hölig K, et al. Treatment of refractory acute GVHD with third-party MSC expanded in platelet lysate-containing medium. Bone Marrow Transplant 2009;43:245.

[97] Senger DR, Perruzzi CA, Papadopoulos-Sergiou A, Van de Water L. Adhesive properties of osteopontin: regulation by a naturally occurring thrombin-cleavage in close proximity to the GRGDS cell-binding domain. Mol Biol Cell 1994;5:565–74.

[98] Schallmoser K, Bartmann C, Rohde E, Reinisch A, Kashofer K, Stadelmeyer E, et al. Human platelet lysate can replace fetal bovine serum for clinical-scale expansion of functional mesenchymal stromal cells. Transfusion 2007;47:1436–46.

[99] Horn P, Bokermann G, Cholewa D, Bork S, Walenda T, Koch C, et al. Impact of individual platelet lysates on isolation and growth of human mesenchymal stromal cells. Cytotherapy 2010;12:888–98.

[100] Capelli C, Domenghini M, Borleri G, Bellavita P, Poma R, Carobbio A, et al. Human platelet lysate allows expansion and clinical grade production of mesenchymal stromal cells from small samples of bone marrow aspirates or marrow filter washouts. Bone Marrow Transplant 2007;40:785.

[101] Holzwarth C, Vaegler M, Gieseke F, Pfister SM, Handgretinger R, Kerst G, et al. Low

physiologic oxygen tensions reduce proliferation and differentiation of human multipotent mesenchymal stromal cells. BMC Cell Biol 2010;11:11.

[102] Walenda G, Hemeda H, Schneider RK, Merkel R, Hoffmann B, Wagner W. Human platelet lysate gel provides a novel three dimensional-matrix for enhanced culture expansion of mesenchymal stromal cells. Tissue Eng Part C Methods 2012;18:924–34.

[103] Doucet C, Ernou I, Zhang Y, Llense J, Begot L, Holy X, et al. Platelet lysates promote mesenchymal stem cell expansion: A safety substitute for animal serum in cell-based therapy applications. J Cell Physiol 2005;205:228–36.

[104] Johansson L, Klinth J, Holmqvist O, Ohlson S. Platelet lysate: a replacement for fetal bovine serum in animal cell culture? Cytotechnology 2003;42:67.

[105] Bernardo ME, Avanzini MA, Perotti C, Cometa AM, Moretta A, Lenta E, et al. Optimization of in vitro expansion of human multipotent mesenchymal stromal cells for cell-therapy approaches: further insights in the search for a fetal calf serum substitute. J Cell Physiol 2007;211:121–30.

[106] Vogel JP, Szalay K, Geiger F, Kramer M, Richter W, Kasten P. Platelet-rich plasma improves expansion of human mesenchymal stem cells and retains differentiation capacity and in vivo bone formation in calcium phosphate ceramics. Platelets 2006;17:462–9.

[107] Mobaraki M, Abbasi R, Omidian Vandchali S, Ghaffari M, Moztarzadeh F, Mozafari M. Corneal Repair and Regeneration: Current Concepts and Future Directions. Front Bioeng Biotechnol 2019;7:135. doi:10.3389/fbioe.2019.00135.

[108] Latifi-Pupovci H, Kuçi Z, Wehner S, Bönig H, Lieberz R, Klingebiel T, et al. In vitro migration and proliferation ("wound healing") potential of mesenchymal stromal cells generated from human CD271+ bone marrow mononuclear cells. J Transl Med 2015;13:315. doi:10.1186/s12967-015-0676-9.

[109] Stute N, Holtz K, Bubenheim M, Lange C, Blake F, Zander AR. Autologous serum for isolation and expansion of human mesenchymal stem cells for clinical use. Exp Hematol 2004;32:1212–25.

[110] Soundararajan M, Kannan S. Fibroblasts and mesenchymal stem cells: Two sides of the same coin? J Cell Physiol 2018;233:9099–109.

[111] Tancharoen W, Aungsuchawan S, Pothacharoen P, Bumroongkit K, Puaninta C, Pangjaidee N, et al. Human platelet lysate as an alternative to fetal bovine serum for culture and endothelial differentiation of human amniotic fluid mesenchymal stem cells. Mol Med Rep 2019;19:5123–32. doi:10.3892/mmr.2019.10182.

[112] Ferraro GA, De Francesco F, Nicoletti G, Paino F, Desiderio V, Tirino V, et al. Human adipose CD34+ CD90+ stem cells and collagen scaffold constructs grafted in vivo fabricate loose connective and adipose tissues. J Cell Biochem 2013;114:1039–49.

[113] Simmons PJ, Torok-Storb B. CD34 expression by stromal precursors in normal human adult bone marrow. Blood 1991;78:2848–53.

[114] Fernandes-Cunha GM, Na K, Putra I, Lee HJ, Hull S, Cheng Y, et al. Corneal wound healing effects of mesenchymal stem cell secretome delivered within a viscoelastic gel carrier. Stem Cells Transl Med 2019;8:478–89.

[115] Mittal SK, Omoto M, Amouzegar A, Sahu A, Rezazadeh A, Katikireddy KR, et al. Restoration of corneal transparency by mesenchymal stem cells. Stem Cell Reports 2016;7:583–90.

[116] Qin Z, Fisher GJ, Voorhees JJ, Quan T. Actin cytoskeleton assembly regulates collagen production via TGF-β type II receptor in human skin fibroblasts. J Cell Mol Med 2018;22:4085–96.

[117] Dolder J Van Den, Mooren R, Vloon APG, Stoelinga PJW, Jansen JA. Platelet-rich plasma: quantification of growth factor levels and the effect on growth and differentiation of rat bone marrow cells. Tissue Eng 2006;12:3067–73.

[118] Bieback K, Hecker A, Kocaömer A, Lannert H, Schallmoser K, Strunk D, et al. Human alternatives to fetal bovine serum for the expansion of mesenchymal stromal cells from bone marrow. Stem Cells 2009;27:2331–41.

[119] Müller I, Kordowich S, Holzwarth C, Spano C, Isensee G, Staiber A, et al. Animal serum-free culture conditions for isolation and expansion of multipotent mesenchymal stromal cells from human BM. Cytotherapy 2006;8:437–44.

[120] Matthyssen S, Dhubhghaill SN, Van Gerwen V, Zakaria N. Xeno-free cultivation of mesenchymal stem cells from the corneal stroma. Invest Ophthalmol Vis Sci 2017;58:2659–65.

[121] Tan KY, Teo KL, Lim JFY, Chen AKL, Reuveny S, Oh SKW. Serum-free media formulations are cell line–specific and require optimization for microcarrier culture. Cytotherapy 2015;17:1152–65.

[122] Jeong W-Y, Kim J-H, Kim C-W. Co-culture of human bone marrow mesenchymal stem cells and macrophages attenuates lipopolysaccharide-induced inflammation in human corneal epithelial cells. Biosci Biotechnol Biochem 2018;82:800–9.

[123] Ito T, Sawada R, Fujiwara Y, Seyama Y, Tsuchiya T. FGF-2 suppresses cellular senescence of human mesenchymal stem cells by down-regulation of TGF-β2. Biochem Biophys Res Commun 2007;359:108–14.

[124] Yang Y, Hsieh T, Ji AT, Hsu W, Liu C, Lee OK, et al. Stromal Tissue Rigidity Promotes Mesenchymal Stem Cell-Mediated Corneal Wound Healing Through the Transforming Growth Factor β Signaling Pathway. Stem Cells 2016;34:2525–35.

[125] Jiang X-X, Zhang YI, Liu B, Zhang S-X, Wu Y, Yu X-D, et al. Human mesenchymal stem cells inhibit differentiation and function of monocyte-derived dendritic cells. Blood 2005;105:4120–6.

[126] Miyagi H, Thomasy SM, Russell P, Murphy CJ. The role of hepatocyte growth factor in corneal wound healing. Exp Eye Res 2018;166:49–55.

[127] Azouna N Ben, Jenhani F, Regaya Z, Berraeis L, Othman T Ben, Ducrocq E, et al. Phenotypical and functional characteristics of mesenchymal stem cells from bone marrow: comparison of culture using different media supplemented with human platelet lysate or fetal bovine serum. Stem Cell Res Ther 2012;3:6.

[128] Tari K, Atashi A, Kaviani S, AkhavanRahnama M, Anbarlou A, Mossahebi-Mohammadi M. Erythropoietin induces production of hepatocyte growth factor from bone marrow mesenchymal stem cells in vitro. Biologicals 2017;45:15–9.

7 Appendix

Faculty PG Training Courses Attended

- Microsoft Word: Creating and Managing Long Documents (2.00 Training Units)
- Mathematics In The Lab (1.00 Training Unit)
- Referencing your Research (1.00 Training Unit)
- Understanding your Research Degree (2.00 Training Units)
- Statistical Test Advisor (1.00 Training Unit)
- Preparing to use NVivo® (1.00 Training Unit)
- Preparing for your Viva (1.00 Training Unit)
- Research Integrity (2.00 Training Units)
- Biomedical Imaging in Research (1.00 Training Unit)
- Introduction to Flow Cytometry (1.00 Training Unit)
- Writing Scientific Abstracts (1.00 Training Unit)
- Microsoft PowerPoint: Creating a Research Poster (1.00 Training Unit)
- Research Data Management (1.00 Training Unit)
- Advanced Presentation Skills for Researchers (2.00 Training Units)
- Research Data Management II (2.00 Training Units)
- Equality and Diversity at Work (0.00 Training Units)